

DEIRA

**A 1-D 3-T hydrodynamic code for simulating
ICF targets driven by fast ion beams**

Version 4

M. BASKO

INSTITUTE FOR THEORETICAL AND EXPERIMENTAL PHYSICS

MOSCOW, 2001

Contents

1	INTRODUCTION	3
2	NOTATION AND UNITS	3
3	DIFFERENTIAL EQUATIONS	5
3.1	Equations in Eulerian Form	5
3.2	Equations in Lagrangean Form with Artificial Viscosity	6
4	BOUNDARY CONDITIONS	8
5	EQUATION OF STATE	9
5.1	Ideal Boltzmann gas	9
5.2	Ideal Fermi-Boltzmann gas	10
6	SOURCES	11
6.1	Driver Energy Deposition	11
6.2	Thermonuclear Burn Rates	11
6.3	Heating by Neutrons	13
7	KINETIC COEFFICIENTS	15
7.1	Electron Heat Conduction, Electrical Resistivity, and Relaxation between the Electron and Ion Temperatures	15
7.2	Radiation Diffusion and Relaxation between the Electron and Radiation Temperatures	18
7.3	Ion Heat Conduction and Viscosity	21
7.4	Diffusion and Relaxation of the Energy of Fast Fusion Products	22
8	FINITE DIFFERENCE SCHEME	25
8.1	Finite Difference Equations	25
8.2	Conservation Laws	28
9	NUMERICAL ALGORITHM	31
10	EVALUATION OF THE TIME STEP	36
11	BLOCK SCHEME OF THE DEIRA CODE	38
12	TEST PROBLEMS	38
12.1	Hydrodynamics	38
12.2	Electron Heat Conduction and Diffusion of Radiation	39
12.3	Diffusion of the Energy of Fast Fusion Products	41
A	Single-fluid dissipative MHD equations derived from the two-fluid Braginskii equations	43
B	Opacity model: version DEIRA-3	43
B.1	General formulae	43
B.2	Basic formulae in the DEIRA units	44
B.3	General formulae for the absorption cross-section	45
B.3.1	Bound-bound and bound-free transitions	45
B.3.2	Free-free transitions	46
B.4	Absorption cross-section in the DEIRA units	46

1 INTRODUCTION

The physical and mathematical model presented below has been formulated with the aim to create a one-dimensional (1-D) numerical code for simulating inertial confinement fusion (ICF) targets driven by beams of fast ions. The target geometry may be of one of the following three types: plane-parallel, cylindrical, and spherical. It is assumed that such a target can be irradiated by ion beams only strictly symmetrically within the prescribed geometry, and that the ions propagate along the target radii. An arbitrary mixture of the deuterium, tritium, helium-3, hydrogen, and boron-11 isotopes can be used as a thermonuclear fuel. In particular, our model includes:

- 1) equations of one-dimensional single-fluid two-temperature (2-T) dissipative magnetohydrodynamics (MHD) with the electron and ion heat conduction and the ion physical viscosity;
- 2) diffusion equation for the axial component of the magnetic field; the MHD option is restricted to the plane-parallel and cylindrical geometries only, and only the magnetic field component perpendicular to the radial direction (i.e. along the cylinder axis in the cylindrical case) is treated;
- 3) diffusion equation for the energy density of radiation in the approximation of one frequency group (the approximation of a separate radiation temperature);
- 4) three diffusion equations for the energy densities of the three species of fast charged fusion products, namely, the 3.5-MeV alpha particles, the 3-MeV protons, and the 14.7-MeV protons;
- 5) four nuclear burn equations for the relative abundances of the deuterium, tritium, ^3He , and ^{11}B isotopes;
- 6) stopping equation for the propagation of fast ions in the approximation of straight-line trajectories.

The energy deposition by slow charged fusion products with short ranges, for which no diffusion equations are solved, is included as a local heat source. For the non-local heating by any of the two sorts of fast neutrons two options are provided: the approximation of first scattering and the approximation of uniform heating; note that in the present model the heating by thermonuclear neutrons is evaluated for the central fuel sphere only.

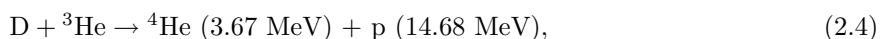
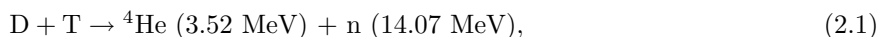
The equation of state is supposed to be given in the form of functions $P_e(V, T_e)$, $P_i(V, T_i)$, $\epsilon_e(V, T_e)$, and $\epsilon_i(V, T_i)$, where P_e , P_i and ϵ_e , ϵ_i are, respectively, the electron and the ion components of the pressure and the internal energy (per unit mass), $V \equiv 1/\rho$ is the specific volume. As a basic option, the equation of state from Ref. [1] is used in a tabular form; it approximates realistic properties of materials in the region of strong coupling, treats properly multiple ionization of atoms (both pressure and thermal), and accounts for the Fermi degeneracy of the electron gas at high densities.

To solve the hydrodynamic equations numerically, an explicit finite-difference scheme with artificial viscosity is used on a Lagrangean mesh. For all the diffusion equations and the heat conduction terms in the hydrodynamic energy equations, a linearized implicit scheme is used, in which the values of heat capacities and transport coefficients are taken from the previous time step.

2 NOTATION AND UNITS

The target to be simulated is assumed to consist of n different planar, cylindrical, or spherical shells (layers). Its geometry is specified by the value of parameter s : $s = 0$ — a planar target, $s = 1$ — a cylindrical target, $s = 2$ — a spherical target. Below we assume that all the quantities should have a subscript corresponding to the shell number, which is omitted for brevity. Except for shells containing thermonuclear fuel, matter in each target shell is assumed to consist of atoms of a single element with atomic number Z and atomic mass A (different shells may have different A and Z). The mean degree of ionization (the mean number of free electrons per atom) is denoted as y , and is assumed to be a known function of density $\rho \equiv 1/V$ and electron temperature T_e .

In target shells containing thermonuclear fuel, the following fusion nuclear reactions are accounted for:



We treat the $\text{H}+^{11}\text{B}$ reaction in a simplified manner by assuming that all the energy of this reaction (8.682 MeV) is released in the form of 3.5 MeV alpha particles.

When describing matter which undergoes nuclear transformations, it is convenient to imagine that it consists of identical “molecules”, with each “molecule” containing X_k atoms (nuclei) of species k . The total number of such imaginary “molecules” in each target shell is arbitrary: it is defined by the initial normalization of concentrations X_k . Later on, in the course of nuclear transformations of one species into another, the number of “molecules” in each Lagrangean mass interval remains constant: only concentrations X_k change. It is convenient to introduce a “molecular” mass A_{mol} defined as

$$A_{mol} = \sum_k X_k A_k. \quad (2.6)$$

This quantity changes only little in the course of nuclear transformations (2.1)–(2.4), and we assume that

$$A_{mol} = \sum_k X_{k0} A_k = \text{constant}, \quad (2.7)$$

where X_{k0} are the initial values of the element concentrations. In addition to A_{mol} , we will need the quantities

$$X_{mol} = \sum_k X_{k0}, \quad Z_{mol} = \sum_k X_{k0} Z_k, \quad \bar{A} = \frac{A_{mol}}{X_{mol}}, \quad (2.8)$$

$$\overline{Z^2}_{mol} = \sum_k X_{k0} Z_k^2, \quad S_{mol} = \sum_k X_{k0} A_k^{-1/2} Z_k^{-2}, \quad (2.9)$$

which allow us to adequately evaluate the transport and relaxation coefficients of a fully ionized plasma in the fuel layers, where matter can be a mixture of different elements. However, since we assume X_{mol} , A_{mol} , Z_{mol} , \dots to be constant, we neglect the effect of the change in the nuclear composition due to nuclear reactions on the values of the transport and relaxation coefficients.

It should be noted here that the present model does not provide for the equation of state (EOS) and rigorous treatment of the transport and relaxation phenomena for mixtures of different elements, i.e. the EOS in each target layer is always calculated for a single element with certain single values of A and Z . Hence, a special attention should be paid to a judicial choice of the A and Z values for a given fuel mixture. For example, if an equimolar mixture of H and ^{11}B is considered, one can choose $Z = 5$ and $A = 9$ — so that a correct value of the total plasma pressure $P_e + P_i$ is recovered for given ρ and $T_e = T_i$ in the fully ionized state. If, on the other hand, a $(\text{H})_1(^{11}\text{B})_{11}$ mixture is considered, a more adequate choice might be $Z = 1$, $A = 11/7$, where again the value of A is chosen such as to obtain a correct value of the total plasma pressure $P_e + P_i$ in the fully ionized state. Note that from the EOS we always obtain a single value of the ionization degree $y = y(\rho, T_e)$ with $0 < y \leq Z$.

In the shells which contain no fuel (IFMFU \emptyset (I)= \emptyset), we assume $X_{mol} = 1$, $A_{mol} = \bar{A} = A$, $Z_{mol} = Z$, $\overline{Z^2}_{mol} = Z^2$, $S_{mol} = A^{-1/2} Z^{-2}$. Then, the general expressions for the number of nuclei n_k of species k , the number of free electrons n_e , and the total number of nuclei n_n per unit volume become

$$n_k = \frac{\rho X_k}{m_A A_{mol}}, \quad n_e = \frac{\rho Z_{mol}}{m_A A_{mol}} \left(\frac{y}{Z} \right), \quad n_n = \frac{\rho}{m_A \bar{A}}, \quad (2.10)$$

where m_A is the atomic mass unit.

In all the equations below, if not stated to the contrary, the following units are used (the DEIRA units):

t	(time)	10^{-8} s = 10 ns
r	(length)	10^{-1} cm = 1 mm
u	(velocity)	10^7 cm s $^{-1}$ = 100 km s $^{-1}$
$\rho = V^{-1}$	(density)	1 g cm $^{-3}$ = 1 mg mm $^{-3}$
B	(magn. field strength)	10^7 Gauss
M, m	(mass)	10^{-3} g mm $^{s-2}$ = 1 mg mm $^{s-2}$
E	(energy)	10^{11} ergs mm $^{s-2}$ = 10 kJ mm $^{s-2}$
P_e, P_i	(pressure)	10^{14} ergs cm $^{-3}$ = 100 Mbar
ϵ_e, ϵ_i	(specific internal energy)	10^{14} ergs g $^{-1}$ = 10 MJ g $^{-1}$

T_e, T_i, T_r	(temperature)	$1 \text{ keV} = 1.1604 \times 10^7 \text{ K}$
q_{ik}	(nuclear reaction rate)	$10^8 \text{ cm}^3 \text{ g}^{-1} \text{ s}^{-1}$
Q_e, Q_i, \dots	(specific heating rate)	$10^{22} \text{ ergs g}^{-1} \text{ s}^{-1} = 1 \text{ TW mg}^{-1}$
$\mathcal{E}_r, \mathcal{E}_\alpha, \dots$	(energy density)	$10^{14} \text{ ergs cm}^{-3}$
ν_{ee}, ν_{ei}	(collision frequency)	10^8 s^{-1}
$\kappa_e, \kappa_i, \kappa_r$	(heat conduction coefficients)	$10^{20} \text{ ergs cm}^{-1} \text{ s}^{-1} \text{ keV}^{-1}$
χ_{ei}, χ_{er}	(temperature relaxation coeff-s)	$10^{22} \text{ ergs g}^{-1} \text{ s}^{-1} \text{ keV}^{-1}$
η_\perp	(specific resistivity)	10^{-8} s
$\eta_{i,sc}, \eta_{i,tn}$	(ion viscosity coeff-s)	$10^6 \text{ g cm}^{-1} \text{ s}^{-1}$
$\chi_\alpha, \chi_{p3}, \chi_{p14}$	(fusion energy relaxation coeff-s)	$10^8 \text{ cm}^3 \text{ g}^{-1} \text{ s}^{-1}$
$d_\alpha, d_{p3}, d_{p14}$	(fusion energy diffusion coeff-s)	$10^6 \text{ cm}^2 \text{ s}^{-1}$
W_b	(beam power)	$10^{19} \text{ ergs s}^{-1} \text{ mm}^{s-2} = 1 \text{ TW mm}^{s-2}$
E_b	(fast ion energy)	$1 \text{ GeV per nucleus}$
S_b	(stopping power)	$1 \text{ GeV mm}^2 \text{ mg}^{-1}$

This system of units is self-consistent in the sense that all the equations below, where the values of dimensional physical constants are not specified as decimal numbers, are valid in any other self-consistent (like CGS) system of units.

3 DIFFERENTIAL EQUATIONS

3.1 Equations in Eulerian Form

We solve the following system of single-fluid dissipative three-temperature (3-T) MHD equations:

$$\frac{\partial \rho}{\partial t} + \frac{1}{r^s} \frac{\partial}{\partial r} (\rho u r^s) = 0, \quad (3.1)$$

$$\begin{aligned} \rho \frac{\partial u}{\partial t} + \rho u \frac{\partial u}{\partial r} + \frac{\partial}{\partial r} \left[P_e + P_i - \eta_{i,sc} \frac{1}{r^s} \frac{\partial}{\partial r} (u r^s) + \frac{B^2}{8\pi} + \frac{\mathcal{E}_r}{3} + \frac{2}{3} (\mathcal{E}_\alpha + \mathcal{E}_{p3} + \mathcal{E}_{p14}) \right] = \\ = \frac{1}{r^{s+1}} \frac{\partial}{\partial r} \left[r^{s+2} \eta_{i,tn} \frac{\partial}{\partial r} \left(\frac{u}{r} \right) \right], \end{aligned} \quad (3.2)$$

$$\begin{aligned} \frac{\partial \epsilon_e}{\partial t} + u \frac{\partial \epsilon_e}{\partial r} + \frac{P_e}{\rho} \frac{1}{r^s} \frac{\partial}{\partial r} (u r^s) = \frac{1}{\rho r^s} \frac{\partial}{\partial r} \left(r^s \hat{\kappa}_e \frac{\partial T_e}{\partial r} \right) + \frac{\eta_\perp}{\rho} \left(\frac{c}{4\pi} \frac{\partial B}{\partial r} \right)^2 - \chi_{ei} (T_e - T_i) - \\ - \chi_{er} (T_e - T_r) + \chi_{e\alpha} \mathcal{E}_\alpha + \chi_{ep3} \mathcal{E}_{p3} + \chi_{ep14} \mathcal{E}_{p14} + Q_{ecl} + Q_{en} + Q_{dr}, \end{aligned} \quad (3.3)$$

$$\begin{aligned} \frac{\partial \epsilon_i}{\partial t} + u \frac{\partial \epsilon_i}{\partial r} + \left[P_i - \eta_{i,sc} \frac{1}{r^s} \frac{\partial}{\partial r} (u r^s) \right] \frac{1}{\rho r^s} \frac{\partial}{\partial r} (u r^s) = \frac{1}{\rho r^s} \frac{\partial}{\partial r} \left(r^s \hat{\kappa}_i \frac{\partial T_i}{\partial r} \right) + \frac{\eta_{i,tn}}{\rho} \left[r \frac{\partial}{\partial r} \left(\frac{u}{r} \right) \right]^2 + \\ + \chi_{ei} (T_e - T_i) + \chi_{i\alpha} \mathcal{E}_\alpha + \chi_{ip3} \mathcal{E}_{p3} + \chi_{ip14} \mathcal{E}_{p14} + Q_{icl} + Q_{in}, \end{aligned} \quad (3.4)$$

$$\frac{\partial \mathcal{E}_r}{\partial t} + u \frac{\partial \mathcal{E}_r}{\partial r} + \frac{4}{3} \mathcal{E}_r \frac{1}{r^s} \frac{\partial}{\partial r} (u r^s) = \frac{1}{r^s} \frac{\partial}{\partial r} \left(r^s \hat{\kappa}_r \frac{\partial T_r}{\partial r} \right) + \rho \chi_{er} (T_e - T_r), \quad (3.5)$$

$$\frac{\partial B}{\partial t} + \frac{1}{r^s} \frac{\partial}{\partial r} (B u r^s) = \frac{c^2}{4\pi} \frac{1}{r^s} \frac{\partial}{\partial r} \left(r^s \eta_\perp \frac{\partial B}{\partial r} \right). \quad (3.6)$$

Here $\eta_{i,sc}$ and $\eta_{i,tn}$ are the coefficients of the ion (physical) viscosity, defined as

$$\eta_{i,sc} = \begin{cases} \frac{1}{3} \eta_0^i + \eta_1^i, & s = 0, \\ \frac{1}{3} \eta_0^i, & s = 1, \\ 0, & s = 2, \end{cases} \quad \eta_{i,tn} = \begin{cases} 0, & s = 0, \\ \eta_1^i, & s = 1, \\ \frac{4}{3} \eta_0^i, & s = 2, \end{cases} \quad (3.7)$$

where η_0^i and η_1^i are the coefficients of the ion viscosity of the magnetized plasmas as defined by Braginskii [2]; without magnetic field $\eta_0^i = \eta_1^i$. Then, $\hat{\kappa}_e$, $\hat{\kappa}_i$, and $\hat{\kappa}_r$ are the electron, κ_e , the ion, κ_i (both transverse with respect to the magnetic field), and radiative, κ_r , heat conduction coefficients corrected for the corresponding flux limits (see §§ 6.1 and 6.2); η_\perp is the transverse electrical resistivity; Q_{ecl} and Q_{icl} are the specific heating rates for plasma electrons and ions by slow charged fusion products which deposit their energy locally, Q_{en} and Q_{in} are the corresponding heating rates by thermonuclear neutrons; Q_{dr} is the specific energy deposition by an external power source (the driver). The energy density of radiation is given by

$$\mathcal{E}_r = a_{SB} T_r^4, \quad (3.8)$$

where $a_{SB} = 4\sigma_{SB}/c \stackrel{\text{D}}{=} 1.372$ is the radiation density constant related to the Stefan-Boltzmann constant σ_{SB} . Here and everywhere below the DEIRA units are used after the symbol $\stackrel{\text{D}}{=}$. Equation (3.6) for the axial magnetic field B has a physical meaning only in the cases of $s = 0$ and $s = 1$. It is derived from the system of two-fluid 2-T Braginskii equations [2] with the Nernst effect being neglected (see Appendix A).

The diffusion equations for volumetric energy densities of the three species of fast charged fusion products are

$$\frac{\partial \mathcal{E}_\alpha}{\partial t} + u \frac{\partial \mathcal{E}_\alpha}{\partial r} + \frac{5}{3} \mathcal{E}_\alpha \frac{1}{r^s} \frac{\partial}{\partial r} (ur^s) + \rho \chi_\alpha \mathcal{E}_\alpha = \frac{1}{r^s} \frac{\partial}{\partial r} \left(r^s d_\alpha \frac{\partial \mathcal{E}_\alpha}{\partial r} \right) + \rho Q_\alpha, \quad (3.9)$$

$$\frac{\partial \mathcal{E}_{p3}}{\partial t} + u \frac{\partial \mathcal{E}_{p3}}{\partial r} + \frac{5}{3} \mathcal{E}_{p3} \frac{1}{r^s} \frac{\partial}{\partial r} (ur^s) + \rho \chi_{p3} \mathcal{E}_{p3} = \frac{1}{r^s} \frac{\partial}{\partial r} \left(r^s d_{p3} \frac{\partial \mathcal{E}_{p3}}{\partial r} \right) + \rho Q_{p3}, \quad (3.10)$$

$$\frac{\partial \mathcal{E}_{p14}}{\partial t} + u \frac{\partial \mathcal{E}_{p14}}{\partial r} + \frac{5}{3} \mathcal{E}_{p14} \frac{1}{r^s} \frac{\partial}{\partial r} (ur^s) + \rho \chi_{p14} \mathcal{E}_{p14} = \frac{1}{r^s} \frac{\partial}{\partial r} \left(r^s d_{p14} \frac{\partial \mathcal{E}_{p14}}{\partial r} \right) + \rho Q_{p14}. \quad (3.11)$$

When calculating the diffusion coefficients d_α , d_{p3} , and d_{p14} , no flux limits are imposed.

The depletion of the thermonuclear fuel is described by the equations

$$\frac{\partial X_D}{\partial t} + u \frac{\partial X_D}{\partial r} = \frac{\rho}{A_{mol}} \left(-X_D X_T q_{DT} - 2X_D^2 q_{DD} - X_D X_{He} q_{DHe} \right), \quad (3.12)$$

$$\frac{\partial X_T}{\partial t} + u \frac{\partial X_T}{\partial r} = \frac{\rho}{A_{mol}} \left(-X_D X_T q_{DT} + \frac{1}{2} X_D^2 q_{DD} \right), \quad (3.13)$$

$$\frac{\partial X_{He}}{\partial t} + u \frac{\partial X_{He}}{\partial r} = \frac{\rho}{A_{mol}} \left(-X_D X_{He} q_{DHe} + \frac{1}{2} X_D^2 q_{DD} \right), \quad (3.14)$$

$$\frac{\partial X_B}{\partial t} + u \frac{\partial X_B}{\partial r} = -\frac{\rho}{A_{mol}} X_B X_H q_{BH} = \frac{\partial X_H}{\partial t} + u \frac{\partial X_H}{\partial r}. \quad (3.15)$$

Here

$$q_{ik} = \frac{\langle \sigma v \rangle_{ik}}{m_A} \quad (3.16)$$

is the rate of $i + k$ nuclear reaction. The two reactions (2.2) and (2.3) are assumed to have the same rate q_{DD} . The total mass of a fuel component k is given by

$$M_k(t) = K(s) \frac{A_k}{A_{mol}} \int_0^R \rho(t, r) X_k(t, r) r^s dr, \quad (3.17)$$

where

$$K(0) = 1, \quad K(1) = 2\pi, \quad K(2) = 4\pi. \quad (3.18)$$

3.2 Equations in Lagrangean Form with Artificial Viscosity

Here we write down the basic differential equations in the form that will be used for constructing the finite difference scheme. At this stage, we introduce the terms with artificial viscosity. As independent Lagrangean variables, we use the time t and the quantity

$$m = \int_0^r \rho r^s dr. \quad (3.19)$$

The coordinate m differs from the mass coordinate by the factor $K(s)$ given in Eq. (3.18). The principal dependent variables are

$$r, \quad u, \quad T_e, \quad T_i, \quad T_r, \quad B, \quad \mathcal{E}_\alpha, \quad \mathcal{E}_{p3}, \quad \mathcal{E}_{p14}, \quad X_D, \quad X_T, \quad X_{He}, \quad X_B. \quad (3.20)$$

Transformation of differential operators from Eulerian to Lagrangean form is accomplished as

$$\frac{\partial}{\partial t} + u \frac{\partial}{\partial r} \rightarrow \frac{\partial}{\partial t}, \quad \frac{\partial}{\partial r} \rightarrow \rho r^s \frac{\partial}{\partial m}. \quad (3.21)$$

The equations of magnetohydrodynamics become:

$$\frac{\partial r}{\partial t} = u, \quad (3.22)$$

$$\begin{aligned} \frac{\partial u}{\partial t} + r^s \frac{\partial}{\partial m} \left[P_{av} + P_e + P_i - \eta_{i,sc} \rho \frac{\partial}{\partial m} (ur^s) + \frac{B^2}{8\pi} + \frac{a_{SB} T_r^4}{3} + \frac{2}{3} (\mathcal{E}_\alpha + \mathcal{E}_{p3} + \mathcal{E}_{p14}) \right] = \\ = \frac{1}{r} \frac{\partial}{\partial m} \left[(\eta_{av,tn} + \eta_{i,tn} \rho r^{2s+2}) \frac{\partial}{\partial m} \left(\frac{u}{r} \right) \right], \end{aligned} \quad (3.23)$$

$$\begin{aligned} \left(\frac{\partial \epsilon_e}{\partial T_e} \right)_V \frac{\partial T_e}{\partial t} + \left[P_e + \left(\frac{\partial \epsilon_e}{\partial V} \right)_{T_e} \right] \frac{\partial (ur^s)}{\partial m} = \frac{\partial}{\partial m} \left(r^s \hat{\kappa}_e \frac{\partial T_e}{\partial r} \right) + \left(\frac{c}{4\pi} \right)^2 \eta_\perp V \left(\frac{\partial B}{\partial r} \right)^2 - \\ - \chi_{ei}(T_e - T_i) - \chi_{er}(T_e - T_r) + \chi_{e\alpha} \mathcal{E}_\alpha + \chi_{ep3} \mathcal{E}_{p3} + \chi_{ep14} \mathcal{E}_{p14} + Q_{ecl} + Q_{en} + Q_{dr}, \end{aligned} \quad (3.24)$$

$$\begin{aligned} \left(\frac{\partial \epsilon_i}{\partial T_i} \right)_V \frac{\partial T_i}{\partial t} + \left[P_{av} + P_i + \left(\frac{\partial \epsilon_i}{\partial V} \right)_{T_i} - \eta_{i,sc} \rho \frac{\partial (ur^s)}{\partial m} \right] \frac{\partial (ur^s)}{\partial m} = \frac{\partial}{\partial m} \left(r^s \hat{\kappa}_i \frac{\partial T_i}{\partial r} \right) + \chi_{ei}(T_e - T_i) + \\ + (\eta_{av,tn} + \eta_{i,tn} \rho r^{2s+2}) \left[\frac{\partial}{\partial m} \left(\frac{u}{r} \right) \right]^2 + \chi_{i\alpha} \mathcal{E}_\alpha + \chi_{ip3} \mathcal{E}_{p3} + \chi_{ip14} \mathcal{E}_{p14} + Q_{icl} + Q_{in}, \end{aligned} \quad (3.25)$$

$$4a_{SB} T_r^3 V \frac{\partial T_r}{\partial t} + \frac{4}{3} a_{SB} T_r^4 \frac{\partial (ur^s)}{\partial m} = \frac{\partial}{\partial m} \left(r^s \hat{\kappa}_r \frac{\partial T_r}{\partial r} \right) + \chi_{er}(T_e - T_r), \quad (3.26)$$

$$\frac{\partial (BV)}{\partial t} = \frac{c^2}{4\pi} \frac{\partial}{\partial m} \left(r^s \eta_\perp \frac{\partial B}{\partial r} \right). \quad (3.27)$$

Diffusion of the energy density of fast fusion products:

$$V \frac{\partial \mathcal{E}_\alpha}{\partial t} + \frac{5}{3} \mathcal{E}_\alpha \frac{\partial (ur^s)}{\partial m} + \chi_\alpha \mathcal{E}_\alpha = \frac{\partial}{\partial m} \left(r^s d_\alpha \frac{\partial \mathcal{E}_\alpha}{\partial r} \right) + Q_\alpha, \quad (3.28)$$

$$V \frac{\partial \mathcal{E}_{p3}}{\partial t} + \frac{5}{3} \mathcal{E}_{p3} \frac{\partial (ur^s)}{\partial m} + \chi_{p3} \mathcal{E}_{p3} = \frac{\partial}{\partial m} \left(r^s d_{p3} \frac{\partial \mathcal{E}_{p3}}{\partial r} \right) + Q_{p3}, \quad (3.29)$$

$$V \frac{\partial \mathcal{E}_{p14}}{\partial t} + \frac{5}{3} \mathcal{E}_{p14} \frac{\partial (ur^s)}{\partial m} + \chi_{p14} \mathcal{E}_{p14} = \frac{\partial}{\partial m} \left(r^s d_{p14} \frac{\partial \mathcal{E}_{p14}}{\partial r} \right) + Q_{p14}. \quad (3.30)$$

Fuel depletion:

$$\frac{\partial X_D}{\partial t} = \frac{1}{V A_{mol}} \left(-X_D X_T q_{DT} - 2X_D^2 q_{DD} - X_D X_{He} q_{DHe} \right), \quad (3.31)$$

$$\frac{\partial X_T}{\partial t} = \frac{1}{V A_{mol}} \left(-X_D X_T q_{DT} + \frac{1}{2} X_D^2 q_{DD} \right), \quad (3.32)$$

$$\frac{\partial X_{He}}{\partial t} = \frac{1}{V A_{mol}} \left(-X_D X_{He} q_{DHe} + \frac{1}{2} X_D^2 q_{DD} \right), \quad (3.33)$$

$$\frac{\partial X_B}{\partial t} = \frac{\partial X_H}{\partial t} = -\frac{1}{V A_{mol}} X_B X_H q_{BH}. \quad (3.34)$$

The specific volume $V \equiv 1/\rho$ (not among the principal dependent variables) is given by

$$V = \frac{1}{s+1} \frac{\partial r^{s+1}}{\partial m}. \quad (3.35)$$

In particular, from Eqs. (3.22) and (3.35) we have

$$\frac{\partial V}{\partial t} = \frac{\partial (ur^s)}{\partial m} \equiv \dot{V}. \quad (3.36)$$

The additive pressure component due to the scalar artificial viscosity is given by

$$P_{av} = -\eta_{av,sc} \frac{\partial (ur^s)}{\partial m} \equiv -\eta_{av,sc} \dot{V}. \quad (3.37)$$

Here $\eta_{av,sc} \geq 0$ and $\eta_{av,tn} \geq 0$ are, respectively, the coefficients of scalar and tensor components of the artificial viscosity [3]. In equations (3.24)–(3.30), the derivative $\frac{\partial}{\partial r}$ should be understood as the operator $\rho r^s \frac{\partial}{\partial m}$.

4 BOUNDARY CONDITIONS

At the inner (left) boundary $r = R_l$ three different types of boundary conditions are envisaged.

1. Fixed center of symmetry, $R_l = u_l = 0$, all diffusion fluxes are zero:

$$u(t, 0) = 0, \quad (4.1)$$

$$\frac{\partial T_e}{\partial r} = \frac{\partial T_i}{\partial r} = \frac{\partial T_r}{\partial r} = \frac{\partial B}{\partial r} = 0, \quad (4.2)$$

$$\frac{\partial \mathcal{E}_\alpha}{\partial r} = \frac{\partial \mathcal{E}_{p3}}{\partial r} = \frac{\partial \mathcal{E}_{p14}}{\partial r} = 0. \quad (4.3)$$

2. A closed void cavity at $0 < r < R_l$ with a prescribed boundary pressure $P_{bl}(t)$; all diffusion fluxes are zero:

$$\frac{\partial T_e}{\partial r} = \frac{\partial T_i}{\partial r} = \frac{\partial T_r}{\partial r} = \frac{\partial B}{\partial r} = 0, \quad (4.4)$$

$$P(t, R_l) = P_{bl}(t) + \frac{1}{3} a_{SB} T_{r,l}^4 + \frac{B_l^2}{8\pi} + \frac{2}{3} (\mathcal{E}_{\alpha,l} + \mathcal{E}_{p3,l} + \mathcal{E}_{p14,l}), \quad (4.5)$$

$$\frac{\partial \mathcal{E}_\alpha}{\partial r} = \frac{\partial \mathcal{E}_{p3}}{\partial r} = \frac{\partial \mathcal{E}_{p14}}{\partial r} = 0. \quad (4.6)$$

Here $T_{r,l}$, B_l , $\mathcal{E}_{\alpha,l}$, \dots , are the values of corresponding physical quantities calculated at $r = R_l + 0$. The condition for the magnetic field B in this case does not appear as obvious, but no other physically more adequate condition can be suggested immediately.

3. An open halfspace at $-\infty < r < R_l$ with prescribed boundary pressure $P_{bl}(t)$, external radiation temperature $T_{rlex}(t)$ and magnetic field $B_{bl}(t)$:

$$\frac{\partial T_e}{\partial r} = \frac{\partial T_i}{\partial r} = 0, \quad (4.7)$$

$$\kappa_r \frac{\partial T_r}{\partial r} = \frac{1}{4} c a_{SB} (T_r^4 - T_{rlex}^4), \quad (4.8)$$

$$P(t, R) = P_{bl}(t) + \frac{1}{3} a_{SB} T_{rlex}^4 + \frac{B_{bl}^2}{8\pi}, \quad (4.9)$$

$$B(t, R) = B_{bl}(t), \quad (4.10)$$

$$\mathcal{E}_\alpha(t, R_l - 0) = \mathcal{E}_{p3}(t, R_l - 0) = \mathcal{E}_{p14}(t, R_l - 0) = 0. \quad (4.11)$$

This latter type of the left boundary condition is possible for plane-parallel targets only.

The conditions at the outer (right) boundary $r = R$ are:

$$\frac{\partial T_e}{\partial r} = 0, \quad \kappa_r \frac{\partial T_r}{\partial r} = \frac{1}{4} c a_{SB} (T_{rex}^4 - T_r^4), \quad (4.12)$$

$$P(t, R) = P_{br}(t) + \frac{1}{3} a_{SB} T_{rex}^4 + \frac{B_{br}^2}{8\pi}, \quad (4.13)$$

$$B(t, R) = B_{br}(t), \quad (4.14)$$

$$\mathcal{E}_\alpha(t, R+0) = \mathcal{E}_{p3}(t, R+0) = \mathcal{E}_{p14}(t, R+0) = 0. \quad (4.15)$$

Here, the right boundary pressure $P_{rb}(t)$, the right boundary magnetic field $B_{br}(t)$, and the right boundary radiation temperature $T_{rex}(t)$ are assumed to be given functions of their arguments. Default values are $P_{bl} = P_{br} = 0$, $T_{rlex} = T_{rex} = 0$, $B_{bl} = B_{br} = B_0 \equiv B(0, r)$.

5 EQUATION OF STATE

Under the equation of state we understand the algorithm for calculating the thermodynamic functions

$$y = y(V, T_e), \quad (5.1)$$

$$P_e = P_e(V, T_e), \quad (5.2)$$

$$P_i = P_i(V, T_i), \quad (5.3)$$

$$\epsilon_e = \epsilon_e(V, T_e), \quad (5.4)$$

$$\epsilon_i = \epsilon_i(V, T_i), \quad (5.5)$$

and their first derivatives. Functions (5.2)–(5.5) must satisfy the following thermodynamic identities and inequalities:

$$\frac{\partial \epsilon_e}{\partial V} = T_e \frac{\partial P_e}{\partial T_e} - P_e, \quad (5.6)$$

$$\frac{\partial \epsilon_i}{\partial V} = T_i \frac{\partial P_i}{\partial T_i} - P_i, \quad (5.7)$$

$$\frac{\partial P_e}{\partial V} + \frac{\partial P_i}{\partial V} < 0, \quad (5.8)$$

$$\frac{\partial \epsilon_e}{\partial T_e} > 0, \quad \frac{\partial \epsilon_i}{\partial T_i} > 0. \quad (5.9)$$

The adiabatic sound velocity u_s is defined by

$$u_s^2 = V \frac{B^2}{4\pi} + \frac{4}{9} V a_{SB} T_r^4 + V^2 \left[-\frac{\partial P_e}{\partial V} - \frac{\partial P_i}{\partial V} + T_e \frac{(\partial P_e / \partial T_e)^2}{\partial \epsilon_e / \partial T_e} + T_i \frac{(\partial P_i / \partial T_i)^2}{\partial \epsilon_i / \partial T_i} \right]. \quad (5.10)$$

As the main option, functions (5.1)–(5.5) are supposed to be given in a tabular form. In such a case, the interpolation algorithm is assumed to maintain the continuity of functions (5.1)–(5.5), while their first derivatives may generally have jumps. In the V, T_e, T_i phase space, there may exist certain restricted domains where inequality (5.8) is violated (domains of thermodynamic instability). In contrast, the inequalities (5.9) must be fulfilled for all $V > 0$, $T_e > 0$, $T_i > 0$.

5.1 Ideal Boltzmann gas

In the simplest case of a Boltzmann gas of free electrons and a mixture of different ion species k with ionization degrees y_k we have

$$P_e = \frac{\rho T_e}{m_A} \frac{\sum_k X_k y_k}{\sum_k X_k A_k} \stackrel{\text{D}}{=} 9.65 \frac{\sum_k X_k y_k}{\sum_k X_k A_k} \frac{T_e}{V} \stackrel{\text{D, fi}}{=} 9.65 \frac{Z_{mol}}{A_{mol}} \frac{T_e}{V}, \quad (5.11)$$

$$P_i = \frac{\rho T_i}{m_A} \frac{\sum_k X_k}{\sum_k X_k A_k} \stackrel{\text{D}}{=} 9.65 \frac{\sum_k X_k}{\sum_k X_k A_k} \frac{T_i}{V} \stackrel{\text{D, fi}}{=} 9.65 \frac{T_i}{\bar{A} V}, \quad (5.12)$$

$$\epsilon_e = \frac{3}{2} P_e V, \quad \epsilon_i = \frac{3}{2} P_i V, \quad (5.13)$$

where the equality sign $\stackrel{\text{D, fi}}{=}$ indicates a particular case of the DEIRA units and full plasma ionization.

5.2 Ideal Fermi-Boltzmann gas

Introduce the mean atomic mass, \bar{A} , the mean number of free electrons per ion, \bar{y} ,

$$\bar{A} = \frac{\sum_k A_k X_k}{\sum_k X_k}, \quad \bar{y} = \frac{\sum_k y_k X_k}{\sum_k X_k}. \quad (5.14)$$

and the following atomic units for the volume V per ion, the temperatures, T_e , T_i , the pressures P_e , P_i , the internal energies E_e , E_i per ion

$$\begin{aligned} [V] &= a_0^3 = 1.4818 \times 10^{-25} \text{ cm}^3, & [T_e] &= [T_i] = e^2/a_0 = 27.21 \text{ eV}, \\ [P_e] &= [P_i] = e^2/a_0^4 = 2.942 \times 10^{14} \text{ ergs/cm}^3, & [E_e] &= [E_i] = e^2/a_0 = 27.21 \text{ eV/ion}. \end{aligned} \quad (5.15)$$

Transformation between the DEIRA and the atomic units is given by

$$\begin{aligned} V_{\text{au}} &= \frac{11.206 \text{ g/cm}^3 \bar{A}}{\rho_{\text{D}}}, & T_{e(i), \text{ au}} &= \frac{T_{e(i), \text{ D}}}{0.02721}, \\ P_{e(i), \text{ D}} &= 2.942 P_{e(i), \text{ au}} & \epsilon_{e(i), \text{ D}} &= 0.2625 \frac{E_{e(i), \text{ au}}}{\bar{A}}. \end{aligned} \quad (5.16)$$

In atomic units, a convenient approximation to the mixture of the non-relativistic ideal Boltzmann gas of ions and the non-relativistic ideal Fermi gas of electrons is given by

$$\psi \equiv \frac{E_F}{T_e} = \frac{1}{2} (3\pi^2)^{2/3} \left(\frac{\bar{y}}{V} \right)^{2/3} \frac{1}{T_e}, \quad (5.17)$$

$$P_e = \frac{1}{5} (3\pi^2)^{2/3} \left(\frac{\bar{y}}{V} \right)^{5/3} + \frac{\bar{y} T_e}{V} \frac{1}{1 + a_F \psi}, \quad P_i = \frac{T_i}{V}, \quad (5.18)$$

$$E_e = \frac{3}{2} V P_e, \quad E_i = \frac{3}{2} V P_i. \quad (5.19)$$

The entropy parameter α , defined as the ratio of the total pressure $P_e(V, T_e) + P_i(V, T_i)$ to the degenerate pressure $P_e(V, 0)$ for the same specific volume V , is given by

$$\alpha = 1 + \frac{5}{2\psi} \left(\frac{T_i}{\bar{y} T_e} + \frac{1}{1 + a_F \psi} \right). \quad (5.20)$$

The electron components of the free energy $F_e(V, T_e)$ and the chemical potential $\mu_e(V, T_e)$ are given by

$$F_e = \bar{y} T_e \left[\frac{3}{5} \psi - \frac{3}{2} \ln \left(1 + \frac{1}{a_F \psi} \right) \right], \quad (5.21)$$

$$\mu_e = \frac{1}{2} (3\pi^2)^{2/3} \left(\frac{\bar{y}}{V} \right)^{2/3} + T_e \left[\frac{1}{1 + a_F \psi} - \frac{3}{2} \ln \left(1 + \frac{1}{a_F \psi} \right) \right]. \quad (5.22)$$

Here a_F is a dimensionless fitting parameter: for $a_F = 0.4$ the error in approximation of the exact Fermi integrals for P_e never exceeds 1.5%, $a_F = 6/\pi^2 = 0.6079$ corresponds to the exact limit of the electron heat capacity at $T_e \rightarrow 0$, $a_F = \frac{2}{3} [6/\exp(2)]^{1/3} = 0.424665$ corresponds to the exact limit of the chemical potential for $\psi \rightarrow 0$.

6 SOURCES

Under the term ‘‘sources’’ we understand non-diffusion and non-relaxation terms on the right-hand sides of Eqs (3.3), (3.4), (3.9)–(3.15), (3.24), (3.25), (3.28)–(3.34).

6.1 Driver Energy Deposition

The driver is defined as an external source of energy. In our case, this is a beam of fast ions propagating normally with respect to spherical ($s = 2$), cylindrical ($s = 1$), or planar ($s = 0$) surfaces in the corresponding geometry. In Eulerian coordinates, the energy of individual ions $E_b(t, r)$ is determined by solving the equation of beam propagation

$$\frac{\partial E_b}{\partial r} = \rho S_b(E_b, \rho, T_e, T_i) \quad (6.1)$$

with the boundary condition $E_b(t, R) = E_{b0}$; here $R = R(t)$ is the outer target radius, $S_b = S_b(E_b, \rho, T_e, T_i)$ is the stopping power of matter (a known function of its arguments [4]). Integration of Eq. (6.1) is conducted from outside ($r = R$) inwards (towards $r = 0$) and can be terminated at a point $r = r_1$ defined by

$$E_b(t, r_1) [\text{GeV}] \leq 10^{-5} A_b, \quad (6.2)$$

where A_b is the atomic mass of the beam ions.

In the present model, we assume for simplicity that the driver energy is transferred exclusively to the electron component of the plasma. The specific heating rate is

$$Q_{dr}(t, r) = \frac{W_b(t)}{K(s)r^s} \frac{S_b(E_b, \rho, T_e, T_i)}{E_{b0}}, \quad (6.3)$$

where $W_b(t)$ [TW mm $^{s-2}$] is the total beam power. As a finite-difference approximation to the heating rate in the j -th mesh interval, we use the following energy conserving expression

$$Q_{dr,j} = \frac{W_b(t)}{K(s)} \frac{E_b(t, r_{j+1}) - E_b(t, r_j)}{E_{b0} \Delta m_j}. \quad (6.4)$$

There is no need to solve Eq. (6.1) at each time step: it should be integrated only after changes in temperatures and density of the irradiated region accumulate to a noticeable level.

6.2 Thermonuclear Burn Rates

All the formulae given below in this section for the thermonuclear reaction rates q and the energy deposition rates Q are in the DEIRA units. The $\langle \sigma v \rangle$ value for each fusion reaction is related to the corresponding q value as

$$\langle \sigma v \rangle_{ik} [\text{cm}^3 \text{s}^{-1}] = 1.66 \times 10^{-16} q_{ik}, \quad (6.5)$$

where q_{ik} is in the DEIRA units.

For the thermonuclear burn rates, the following approximate formulae [6] are used

$$q_{DT} \stackrel{\text{D}}{=} 1.58 \times 10^4 T_i^{-2/3} \left\{ (1 + 0.16 T_i) \exp \left[-\frac{19.98}{T_i^{1/3}} - \left(\frac{T_i}{10.34} \right)^2 \right] + 0.0108 \exp \left(-\frac{45.07}{T_i} \right) \right\}, \quad (6.6)$$

$$q_{DD} \stackrel{\text{D}}{=} 81.4 T_i^{-2/3} (1 + 0.01 T_i) \exp \left(-\frac{18.81}{T_i^{1/3}} \right), \quad (6.7)$$

$$q_{DHe} \stackrel{\text{D}}{=} 1.3 \times 10^4 T_i^{-2/3} (1 + 5 \times 10^{-4} T_i^2) \exp \left[-\frac{31.72}{T_i^{1/3}} - \left(\frac{T_i}{27.14} \right)^2 \right] + 40.5 T_i^{-1/2} \exp \left(-\frac{148.2}{T_i} \right), \quad (6.8)$$

$$\begin{aligned}
q_{BH} \stackrel{D}{=} & 5.05 \times 10^4 T_i^{-2/3} \left(1 + 0.008 T_i^{1/3} + 0.063 T_i^{2/3} + 0.0034 T_i + 0.0056 T_i^{4/3} + \right. \\
& \left. + 7.9 \times 10^{-4} T_i^{5/3} \right) \exp \left[-\frac{53.423}{T_i^{1/3}} - \left(\frac{T_i}{174.06} \right)^2 \right] + \\
& + 59.2 T_i^{-3/2} \exp \left[-\frac{149.33}{T_i} \right] + 6.51 \times 10^4 T_i^{-3/2} \exp \left[-\frac{618.45}{T_i} \right] + \\
& + 333.6 T_i^{-2/3} \exp \left[-\frac{1094}{T_i} \right]. \tag{6.9}
\end{aligned}$$

Formulae (6.6)-(6.8) approximate more lengthy expressions [like Eq. (6.9)] from Ref. [6] to an accuracy of about 10%, which is the accuracy of the original formulae in Ref. [6]. It is assumed that each of the two reactions (2.2) and (2.3) occurs with the same rate (6.7).

Recently [27] a new (more accurate?) approximation for the H+B reaction was proposed,

$$\langle \sigma v \rangle_{BH} = \langle \sigma v \rangle_{BH,nr} + 5.41 \times 10^{-15} T_i^{-3/2} \exp \left(-\frac{148.0}{T_i} \right), \tag{6.10}$$

where for $T_i < 70$ keV

$$\langle \sigma v \rangle_{BH,nr} = 4.455 \times 10^{-16} S T_i^{-2/3} \exp \left(-\frac{53.42365}{T_i^{1/3}} \right), \tag{6.11}$$

$$S = 1.97 \times 10^5 \left(1 + \frac{5T_i}{36E_0} \right) + 240 \left(E_0 + \frac{35}{36} T_i \right) + 0.231 \left(E_0^2 + \frac{89}{36} E_0 T_i \right), \tag{6.12}$$

$$E_0 = 17.8079 T_i^{2/3}, \tag{6.13}$$

and for $50 \text{ keV} < T_i < 500 \text{ keV}$

$$\langle \sigma v \rangle_{BH,nr} = 6.3825 \times 10^{-13} \zeta^{-5/6} \tau^2 \exp \left(-3\zeta^{1/3} \tau \right), \tag{6.14}$$

$$\tau = \frac{17.8079}{T_i^{1/3}}, \tag{6.15}$$

$$\zeta = 1 - T_i \frac{-5.9357 \times 10^{-2} + T_i(1.0404 \times 10^{-3} - 9.1653 \times 10^{-6} T_i)}{1 + T_i [0.20165 + T_i(2.7621 \times 10^{-3} + 9.8305 \times 10^{-7} T_i)]}. \tag{6.16}$$

The specific rate of local heating by slow charged products (helium-3 and tritium) of thermonuclear reactions is

$$Q_{ecl} \stackrel{D}{=} \frac{\rho}{A_{mol}^2} \frac{1}{2} X_D^2 q_{DD} (0.97 \times 10^4 f_{eHe} + 0.79 \times 10^4 f_{eT}), \tag{6.17}$$

$$Q_{icl} \stackrel{D}{=} \frac{\rho}{A_{mol}^2} \frac{1}{2} X_D^2 q_{DD} [0.97 \times 10^4 (1 - f_{eHe}) + 0.79 \times 10^4 (1 - f_{eT})], \tag{6.18}$$

$$f_{eHe} \stackrel{D}{=} \frac{5.6}{5.6 + T_e}, \quad f_{eT} \stackrel{D}{=} \frac{7.0}{7.0 + T_e}. \tag{6.19}$$

The total specific power of the local energy deposition by slow charged fusion products is

$$Q_{cl} = Q_{ecl} + Q_{icl} \stackrel{D}{=} 1.76 \times 10^4 \frac{\rho}{A_{mol}^2} \frac{1}{2} X_D^2 q_{DD}. \tag{6.20}$$

The specific powers of non-local energy sources of charged fusion products (source terms in the corresponding diffusion equations for the energy densities of these products) are

$$Q_\alpha \stackrel{D}{=} \frac{\rho}{A_{mol}^2} (3.40 \times 10^4 X_D X_T q_{DT} + 3.54 \times 10^4 X_D X_{He} q_{DHe} +$$

$$+8.38 \times 10^4 X_B X_H q_{BH}), \quad (6.21)$$

$$Q_{p3} \stackrel{D}{=} \frac{\rho}{A_{mol}^2} 2.91 \times 10^4 \frac{1}{2} X_D^2 q_{DD}, \quad (6.22)$$

$$Q_{p14} \stackrel{D}{=} \frac{\rho}{A_{mol}^2} 14.16 \times 10^4 X_D X_{He} q_{DHe}. \quad (6.23)$$

The total specific power of thermonuclear energy sources (including the energy of neutrons) is given by

$$Q_{fus} \stackrel{D}{=} \frac{\rho}{A_{mol}^2} \left(1.70 \times 10^5 X_D X_T q_{DT} + 7.04 \times 10^4 \frac{1}{2} X_D^2 q_{DD} + \right. \\ \left. + 1.77 \times 10^5 X_D X_{He} q_{DHe} + 8.38 \times 10^4 X_B X_H q_{BH} \right). \quad (6.24)$$

6.3 Heating by Neutrons

Heating by thermonuclear neutrons is evaluated only for target shells which contain thermonuclear fuel. Temporal retardation of the neutron flux is neglected. The specific neutron energy deposition rates are written as

$$Q_{en} = Q_{n14} f_{en14} + Q_{n2} f_{en2}, \quad (6.25)$$

$$Q_{in} = Q_{n14}(1 - f_{en14}) + Q_{n2}(1 - f_{en2}). \quad (6.26)$$

Here Q_{n14} and Q_{n2} are the total specific deposition powers by 14-MeV [reaction (2.1)] and 2.5-MeV [reaction (2.2)] neutrons. Coefficients $0 < f_{en14} < 1$ and $0 < f_{en2} < 1$ represent the energy fractions left by the recoil nuclei in the plasma electrons. Similar to Eq. (6.19), we approximate them as

$$f_{en14} \stackrel{D}{=} [1 + (1 + \bar{A})^2 T_e / 750]^{-1}, \quad (6.27)$$

$$f_{en2} \stackrel{D}{=} [1 + (1 + \bar{A})^2 T_e / 130]^{-1}. \quad (6.28)$$

When fuel is present only in the central target region $0 < r < R_{fu}$ (which may consist of more than one shell, each of the quantities Q_{n14} and Q_{n2} can be evaluated according to one of the following three options.

I. Approximation of the first scattering. This approximation can be self-consistently implemented only in the cylindrical and spherical geometries:

$$Q_{n14}(r) \stackrel{D}{=} \frac{1100}{A} \int_0^{R_{fu}} q_{DT}(r') X_D(r') X_T(r') \left[\frac{\rho(r')}{A_{mol}} \right]^2 \mathcal{G}(r, r') dr', \quad (6.29)$$

$$Q_{n2}(r) \stackrel{D}{=} \frac{650}{A} \int_0^{R_{fu}} \frac{1}{2} q_{DD}(r') \left[\frac{X_D(r') \rho(r')}{A_{mol}} \right]^2 \mathcal{G}(r, r') dr', \quad (6.30)$$

where

$$\mathcal{G}(r, r') = \begin{cases} \frac{2r'}{r+r'} \mathcal{K} \left(\frac{2\sqrt{rr'}}{r+r'} \right), & s = 1, \\ \frac{r'}{r} \ln \left| \frac{r+r'}{r-r'} \right|, & s = 2, \end{cases} \quad (6.31)$$

$\mathcal{K}(x)$ is the full elliptic integral of the first kind. Constants 1100 and 650 in front of the integrals in Eqs (6.29) and (6.30) are the numerical values of the quantity

$$\frac{1}{2} \frac{A_D}{\langle \rho l \rangle_D} \left\langle \frac{\Delta E_n}{m_A} \right\rangle_D,$$

where $\left\langle \frac{\Delta E_n}{m_A} \right\rangle_D$ is the mean energy loss (in units 10^{14} ergs/g) by neutrons after the first scattering off a deuterium nucleus, $\langle \rho l \rangle_D$ is the mean range of neutrons (in units mg/mm^2) in pure deuterium (admixture

of tritium has no practical effect on the value of this constant). Strictly speaking, Eqs (6.29) and (6.30) are valid in the limits $\tau_{n14} \ll 1$, $\tau_{n2} \ll 1$ only [definitions of τ_{n14} and τ_{n2} are given below in Eq. (6.36)], and it should be remembered that for $\tau_{n14} > 1$ ($\tau_{n2} > 1$) the neutron heating calculated from Eq. (6.29) [(6.30)] can exceed even the total thermonuclear energy liberation (6.24).

II. Local deposition. When the optical thickness of the fuel with respect to neutron scattering is large, $\tau_{n14} \gg 1$, $\tau_{n2} \gg 1$, the neutron heating can be estimated in the local approximation

$$Q_{n14} \stackrel{D}{=} 13.6 \times 10^4 q_{DT} X_D X_T \frac{\rho}{A_{mol}^2}, \quad (6.32)$$

$$Q_{n2} \stackrel{D}{=} 2.37 \times 10^4 \frac{1}{2} q_{DD} X_D^2 \frac{\rho}{A_{mol}^2}. \quad (6.33)$$

III. Approximation of a uniform spread. In this approximation we assume that the total fraction of the neutron energy left inside the fuel region $0 < r < R_{fu}$ is spread uniformly over the fuel mass in this region; we evaluate this fraction as $(1 + \tau_0/\tau_n)^{-1}$, where τ_0 is a constant, and τ_n is the optical thickness of the fuel region $0 < r < R_{fu}$ with respect to the scattering of the corresponding neutron species. The value of τ_0 can be calculated in the limit $\tau_n \rightarrow 0$, when Eqs (6.29) and (6.30) become valid. As a result, we obtain $\tau_0 = 3.0$ for a neutron source in the center of a fuel sphere, $\tau_0 = 4.0$ for a neutron source spread uniformly over a fuel sphere, and $\tau_0 = 6.0$ for a neutron source along the outer rim of a fuel sphere. Assuming $\tau_0 = 4.0$ as a reasonable compromise, we obtain

$$Q_{n14} \stackrel{D}{=} 13.6 \times 10^4 \frac{\tau_{n14}}{\tau_{n14} + 4.0} \frac{\int_0^{R_{fu}} q_{DT} X_D X_T (\rho/A_{mol})^2 r^s dr}{\int_0^{R_{fu}} \rho r^s dr}, \quad (6.34)$$

$$Q_{n2} \stackrel{D}{=} 2.37 \times 10^4 \frac{\tau_{n2}}{\tau_{n2} + 4.0} \frac{\frac{1}{2} \int_0^{R_{fu}} q_{DD} (\rho X_D/A_{mol})^2 r^s dr}{\int_0^{R_{fu}} \rho r^s dr}, \quad (6.35)$$

where

$$\tau_{n14} \stackrel{D}{=} \frac{1}{20} \int_0^{R_{fu}} \frac{\rho}{A} dr, \quad \tau_{n2} \stackrel{D}{=} \frac{1}{6.5} \int_0^{R_{fu}} \frac{\rho}{A} dr. \quad (6.36)$$

IV. Approximation of a diffusion-profile spread (version 4.2 of 2006.11.24). This approximation has been implemented for 14-MeV neutrons only, and for the spherical ($s = 2$) geometry only. In this approximation we assume that all the energy of 14-MeV neutrons, generated in the fuel sphere $0 < r < R_{fu}$, is spread over the fuel mass according to the diffusion profile $\phi(\tau)$, namely,

$$Q_{n14}(r) \stackrel{D}{=} \frac{13.6 \times 10^4}{20\bar{A}} \left[\int_0^{R_{fu}} q_{DT} X_D X_T \left(\frac{\rho}{A_{mol}} \right)^2 r^2 dr \right] \frac{\tau^2}{r^2} \phi(\tau), \quad (6.37)$$

where

$$\tau(r) \stackrel{D}{=} \frac{1}{20} \int_0^r \frac{\rho}{A} dr, \quad (6.38)$$

and

$$\phi(\tau) = \frac{3}{\tau_0^3} \begin{cases} 1 - \frac{1 + \tau_0}{2\tau} (e^{\tau - \tau_0} - e^{-\tau - \tau_0}), & 0 < \tau < \tau_0, \\ \frac{\tau_0 - 1 + (\tau_0 + 1)e^{-2\tau_0}}{2\tau} e^{\tau_0 - \tau}, & \tau > \tau_0. \end{cases} \quad (6.39)$$

The profile $\phi(\tau)$ has one free parameter τ_0 . For any $\tau_0 > 0$ it is normalized by the condition

$$\int_0^\infty \phi(\tau) \tau^2 d\tau = 1. \quad (6.40)$$

By its meaning from the derivation of the diffusion profile, τ_0 is the “optical” radius of the 14-MeV generating fuel core. In the DEIRA code the value of τ_0 is determined as the position (along the τ coordinate) where the function

$$q_{DT} X_D X_T \left(\frac{\rho}{A_{mol}} \right)^2 r^2 \quad (6.41)$$

drops by a factor 2 from its maximum value; if the function (6.41) is uniform to within a factor 2, then $\tau_0 = \tau_{n14}$ is the optical thickness for 14-MeV neutrons of the entire fuel sphere $0 < r < R_{fu}$.

In the framework of the present model, the neutron heating of non-central fuel shells can only be evaluated in the local approximation (6.32), (6.33) (or neglected altogether).

7 KINETIC COEFFICIENTS

The above equations of magnetohydrodynamics, and of radiation and fast-product energy diffusion contain the following kinetic coefficients: κ_e , κ_i , κ_r , χ_{ei} , χ_{er} are the coefficients of transverse (with respect to the magnetic field) heat conduction and temperature relaxation; η_0^i and η_1^i are the ion (physical) viscosity coefficients; η_{\perp} is the transverse electrical conductivity coefficient; d_{α} , d_{p3} , d_{p14} , $\chi_{\alpha} = \chi_{e\alpha} + \chi_{i\alpha}$, $\chi_{p3} = \chi_{ep3} + \chi_{ip3}$, $\chi_{p14} = \chi_{ep14} + \chi_{ip14}$ are the coefficients of diffusion and relaxation of the energy of fast fusion products. The formulae for these coefficients given below are based on the expressions published earlier in Refs [2, 7, 5, 8, 9, 10].

7.1 Electron Heat Conduction, Electrical Resistivity, and Relaxation between the Electron and Ion Temperatures

Following Ref. [11], we define the limiting heat flux due to the electron heat conduction as

$$F_{em} = f_{\kappa e} n_e \left(\frac{T_e}{m_e} \right)^{1/2} T_e = 1.28 \times 10^3 f_{\kappa e} \left(\frac{\rho y Z_{mol}}{Z A_{mol}} \right) T_e^{3/2}, \quad (7.1)$$

where $f_{\kappa e}$ is the flux limiting factor; regularly, $f_{\kappa e} = 0.5$ is assumed. Accordingly, the coefficient of the electron heat conduction corrected for the flux limit is defined as

$$\hat{\kappa}_e = \min \left\{ \kappa_e; \frac{F_{em}}{|\nabla T_e|} \right\}. \quad (7.2)$$

Here we only need the transverse (with respect to the magnetic field) conduction coefficient κ_e . Following Ref. [10], we write it in the form

$$\kappa_e = \frac{n_e T_e}{m_e \nu_{\kappa en}} \Gamma_1(x_{\kappa ei}, w_{\kappa e}) \stackrel{D}{=} 1.697 \times 10^5 \left(\frac{\rho y Z_{mol}}{Z A_{mol}} \right) \frac{T_e}{\nu_{\kappa en}} \Gamma_1(x_{\kappa ei}, w_{\kappa e}), \quad (7.3)$$

where

$$\Gamma_1(x, w) = \frac{x^2 \Gamma_{1,1}(w) + \Gamma_{1,2}(w)}{x^4 + x^2 \Gamma_{7,1}(w) + [\Gamma_{7,2}(w)]^2}, \quad (7.4)$$

$$\Gamma_{1,1}(w) = \Gamma_{1,10} + \Gamma_{1,11} w, \quad (7.5)$$

$$\Gamma_{1,2}(w) = \Gamma_{1,20} + \Gamma_{1,21} w + \Gamma_{1,22} w^2 + \Gamma_{1,23} w^3, \quad (7.6)$$

$$\Gamma_{7,1}(w) = \Gamma_{7,10} + \Gamma_{7,11} w + \Gamma_{7,12} w^2, \quad (7.7)$$

$$\Gamma_{7,2}(w) = \Gamma_{7,20} + \Gamma_{7,21} w + \Gamma_{7,22} w^2, \quad (7.8)$$

$$x_{\kappa ei} = \frac{eB}{m_e c \nu_{\kappa en}} \stackrel{D}{=} 1.759 \times 10^6 \frac{B}{\nu_{\kappa en}}. \quad (7.9)$$

Here

$$w_{\kappa e} = \frac{\nu_{\kappa ee}}{\nu_{\kappa en}} \quad (7.10)$$

is the ratio between the frequencies of the electron-electron and electron-ion collisions. We include the effects of the electron degeneracy and of the electron-atom scattering by writing

$$\begin{aligned}\nu_{\kappa ee} &= \frac{4\sqrt{\pi}}{3} \frac{e^4 n_e L_{ee}}{m_e^{1/2} T_e [T_e^2 + (\beta_{\kappa ee} E_F)^2]^{1/4}} \stackrel{\text{D}}{=} \\ &\stackrel{\text{D}}{=} 3.914 \times 10^5 \left(\frac{\rho y Z_{mol}}{Z A_{mol}} \right) \frac{L_{ee}}{T_e [T_e^2 + (\beta_{\kappa ee} E_F)^2]^{1/4}},\end{aligned}\quad (7.11)$$

$$\nu_{\kappa en} = \nu_{ei}(\beta_{\kappa ei}) + \nu_{ea}, \quad (7.12)$$

$$\begin{aligned}\nu_{ei}(\beta) &= \frac{4\sqrt{2\pi}}{3} \frac{e^4 n_i y^2 L_{ei}}{m_e^{1/2} [T_e^2 + (\beta E_F)^2]^{3/4}} \stackrel{\text{D}}{=} \\ &\stackrel{\text{D}}{=} 5.536 \times 10^5 \left(\frac{\rho \bar{Z}^2_{mol}}{Z^2 A_{mol}} \right) \frac{L_{ei}}{[T_e^2 + (\beta E_F)^2]^{3/4}} \times \begin{cases} y, & y < 1, \\ y^2, & y \geq 1, \end{cases}\end{aligned}\quad (7.13)$$

$$\begin{aligned}\nu_{ea} &= \sigma_{ea} n_a \left(\frac{T_F}{m_e} \right)^{1/2} \exp[-(E_F/13 \text{ eV})^2] \stackrel{\text{D}}{=} \\ &\stackrel{\text{D}}{=} 7.987 \times 10^9 \sqrt{T_F} \frac{\rho}{A} \exp[-(E_F/0.013)^2] \times \begin{cases} (1-y), & y < 1, \\ 0, & y \geq 1. \end{cases}\end{aligned}\quad (7.14)$$

For the electron-atom collisions we simply assume a fixed cross-section of $\sigma_{ea} = 10^{-15} \text{ cm}^2$.

In the non-degenerate limit $E_F = 0$, the definitions (7.11) and (7.13) of the electron-electron and electron-ion collision frequencies coincide with those in Refs. [2] and [10]. We calculate the values of the interpolation coefficients

$$\beta_{\kappa ee} = \left[\frac{20\pi^3 \sqrt{2\pi}}{216} \frac{(\Gamma_{7,22})^2}{\Gamma_{1,23}} \right]^2 = 3.394, \quad (7.15)$$

$$\beta_{\kappa ei} = \pi \left[\frac{4}{9} \frac{(\Gamma_{7,20})^2}{\Gamma_{1,20}} \right]^{2/3} = 0.3402, \quad (7.16)$$

from the condition that in the limit of strong degeneracy, $E_F \gg T_e$, the above formulae yield the expressions for κ_{ei} (in the limit of $w \rightarrow 0$) and κ_{ee} (in the limit of $w \rightarrow \infty$) calculated by Lee [12] and Lampe [13].

The transverse electrical resistivity is given by [10]

$$\eta_{\perp} = \frac{m_e \nu_{\eta en}}{e^2 n_e} [1 - \Gamma_5(x_{\eta ei}, w_{\eta})] \stackrel{\text{D}}{=} 6.556 \times 10^{-17} \left(\frac{Z A_{mol}}{\rho y Z_{mol}} \right) \nu_{\eta en} [1 - \Gamma_5(x_{\eta ei}, w_{\eta})], \quad (7.17)$$

where

$$\Gamma_5(x, w) = \frac{x^2 \Gamma_{5,1}(w) + \Gamma_{5,2}(w)}{x^4 + x^2 \Gamma_{7,1}(w) + [\Gamma_{7,2}(w)]^2}, \quad (7.18)$$

$$\Gamma_{5,1}(w) = \Gamma_{5,10} + \Gamma_{5,11} w, \quad (7.19)$$

$$\Gamma_{5,2}(w) = \Gamma_{5,20} + \Gamma_{5,21} w + \Gamma_{5,22} w^2 + \Gamma_{5,23} w^3, \quad (7.20)$$

$$x_{\eta ei} = \frac{eB}{m_e c \nu_{\eta en}} \stackrel{\text{D}}{=} 1.759 \times 10^6 \frac{B}{\nu_{\eta en}}, \quad (7.21)$$

$$w_{\eta} = \frac{\nu_{\eta ee}}{\nu_{\eta en}} = \frac{\nu_{\kappa ee}}{\nu_{\eta en}}, \quad (7.22)$$

$$\nu_{\eta en} = \nu_{ei}(\beta_{\eta ei}) + \nu_{ea}. \quad (7.23)$$

The interpolation coefficient

$$\beta_{\eta ei} = \left[\frac{4}{3\sqrt{\pi}} \left(1 - \frac{\Gamma_{5,20}}{(\Gamma_{7,20})^2} \right) \right]^{2/3} = 0.3665 \quad (7.24)$$

is chosen such as to give the correct degenerate limit calculated by Lampe [14] for $\nu_{\eta ee} = 0$. We assume for simplicity $\nu_{\eta ee} = \nu_{\kappa ee}$ because the contribution of the electron-electron collisions to resistivity can be neglected in the degenerate limit [14].

The coefficient χ_{ei} of the electron-ion temperature relaxation, defined such that $\rho\chi_{ei}(T_e - T_i)$ [ergs cm⁻³ s⁻¹] is the rate of the energy transfer from the electrons to the ions per unit plasma volume, is given by [2]

$$\chi_{ei} = \frac{1}{\rho} \frac{3m_e}{m_i} n_e \nu_{\chi en} \stackrel{D}{=} 1.588 \times 10^{-2} \left(\frac{Z_{mol} y}{AA_{mol} Z} \right) \nu_{\chi en}. \quad (7.25)$$

Here, similar to Eqs. (7.12) and (7.23), the collision frequency is defined as

$$\nu_{\chi en} = \nu_{ei}(\beta_{\chi ei}) + \nu_{ea}, \quad (7.26)$$

where the interpolation coefficient

$$\beta_{\chi ei} = \left(\frac{4}{3\sqrt{\pi}} \right)^{2/3} = 0.8271 \quad (7.27)$$

is chosen such as to yield the correct degenerate limit calculated in Refs. [15, 16]. Table 1 lists the values of coefficients — which are all rational fractions — as calculated in Ref. [10].

Table 1: The values of $\Gamma_{i,jk}$ as calculated in Ref. [10]

	$j = 1$			$j = 2$			
	$k = 0$	$k = 1$	$k = 2$	$k = 0$	$k = 1$	$k = 2$	$k = 3$
$i = 1$	$\frac{13}{4}$	2	0	$\frac{93961}{4900 \cdot 16}$	$\frac{37574}{4900}$	$\frac{42768}{4900}$	$\frac{1296}{490}$
2	$\frac{5}{2}$	0	0	$\frac{320797}{490 \cdot 64}$	$\frac{632025}{49000}$	$\frac{2277}{490}$	0
3	$\frac{2127}{560}$	$\frac{1032}{560}$	0	$\frac{7161}{49000}$	$\frac{59394}{49000}$	$\frac{127728}{49000}$	$\frac{5184}{4900}$
4	$\frac{3}{2}$	0	0	$\frac{429675}{490000}$	$\frac{100665}{49000}$	$\frac{7092}{4900}$	0
5	$\frac{363033}{4900 \cdot 16}$	$\frac{123705}{49000}$	0	$\frac{33201}{490000}$	$\frac{341064}{490000}$	$\frac{957888}{490000}$	$\frac{41472}{49000}$
6	$\frac{477}{280}$	0	0	$\frac{4608}{49000}$	$\frac{21744}{49000}$	$\frac{36432}{49000}$	0
7	$\frac{586601}{4900 \cdot 16}$	$\frac{41269}{4900}$	$\frac{13252}{4900}$	$\frac{31}{100}$	$\frac{1208}{700}$	$\frac{576}{700}$	0
8	$\frac{6}{5}$	$\frac{6}{5}$	0	$\frac{58752}{49000}$	$\frac{243252}{49000}$	$\frac{294051}{49000}$	$\frac{10947}{4900}$
9	1	0	0	$\frac{1494}{490}$	$\frac{25446}{4900}$	$\frac{46561}{4900 \cdot 4}$	0
10	$\frac{26532}{4900}$	$\frac{44094}{4900}$	$\frac{79321}{4900 \cdot 4}$	$\frac{576}{700}$	$\frac{1806}{700}$	$\frac{1068}{700}$	0

The Coulomb logarithms are approximated as

$$L_{ei} = \ln \left[1 + \frac{g_{fit,\kappa} \Lambda_{ei}}{1 + (6.5g_{fit,\kappa} \Lambda_{ei})^{-1}} \right], \quad (7.28)$$

$$L_{ee} = \frac{2}{3} \ln \left[1 + \frac{\Lambda_{ee}^{3/2}}{1 + (8.5\Lambda_{ee}^{3/2})^{-1}} \right], \quad (7.29)$$

Table 2: The values of the fit parameter $g_{fit,\kappa}$

Element	Z	$g_{fit,\kappa}$
Cu	29	3.0
Au	79	6.0

where

$$\Lambda_{ei} = \frac{3 T_F D_{ei}}{e^2 [y^2 + \frac{3}{4} (T_F \hbar^2 / m_e e^4)]^{1/2}} \stackrel{\text{D}}{=} 631 T_F [D_{ei}^{-2} (y^2 + 27.56 T_F)]^{-1/2}, \quad (7.30)$$

$$\Lambda_{ee} = \frac{\frac{3}{2} T_e D_{ee}}{e^2 [1 + \frac{3}{4} (T_F \hbar^2 / m_e e^4)]^{1/2}} \stackrel{\text{D}}{=} 315.5 T_e [D_{ee}^{-2} (1 + 27.56 T_F)]^{-1/2}, \quad (7.31)$$

$$D_{ei}^{-2} = D_{ee}^{-2} + \frac{4\pi e^2 n_i y^2}{T_i} \stackrel{\text{D}}{=} D_{ee}^{-2} + \frac{\rho \bar{Z}^2_{mol}}{A_{mol}} \left(\frac{y}{Z}\right)^2 \frac{1}{T_i}, \quad (7.32)$$

$$D_{ee}^{-2} = \frac{4\pi e^2 n_e}{T_F} \stackrel{\text{D}}{=} \frac{\rho y Z_{mol}}{Z A_{mol} T_F}, \quad T_F = \left[T_e^2 + \left(\frac{2}{3} E_F\right)^2 \right]^{1/2}, \quad (7.33)$$

$$E_F = \frac{\hbar^2}{2 m_e} (3\pi^2 n_e)^{2/3} \stackrel{\text{D}}{=} 0.026 \left(\frac{\rho y Z_{mol}}{Z A_{mol}}\right)^{2/3}, \quad \theta_e = \frac{T_e}{E_F}. \quad (7.34)$$

Eqs (7.28) and (7.29) are written such as to give $\ln \Lambda_{ei}$ ($\ln \Lambda_{ee}$) in the limit $\Lambda_{ei} \gg 1$ ($\Lambda_{ee} \gg 1$), and to reproduce (for $g_{fit,\kappa} = 1$) correct asymptotical behaviors in the limits $\Lambda_{ei} \ll 1$ and $\Lambda_{ee} \ll 1$ as calculated in Refs [17] and [14]. The parameter $g_{fit,\kappa}$ (see Table 2) is introduced in order to fit the experimental values of κ_e and η_{\perp} in metals at room temperatures; its default value is $g_{fit,\kappa} = 1$. Expressions (7.30) and (7.31) are taken from Ref. [18]; Eq. (7.31) agrees well in all limiting cases with formulae used in Ref. [19]. Note that, when written in the DEIRA units, the quantities D_{ei} and D_{ee} in Eqs (7.30)–(7.33) are redefined such as to contain no numerical factors.

7.2 Radiation Diffusion and Relaxation between the Electron and Radiation Temperatures

The coefficient of radiative heat conduction $\hat{\kappa}_r$, corrected for the flux limit, is defined as

$$\hat{\kappa}_r = \min \left\{ \kappa_r; \frac{F_{rm}}{|\nabla T_r|} \right\}, \quad (7.35)$$

where

$$F_{rm} = f_{\kappa r} a_{SB} c T_r^4 \quad (7.36)$$

is the limiting flux for the radiation energy, and $0 < f_{\kappa r} < 1$ is a flux limiting factor; regularly, the value $f_{\kappa r} = 0.5$ is assumed, which would be adequate for the propagation of a steep plane-parallel radiation front.

The uncorrected coefficient of radiative heat conduction κ_r is expressed in terms of the Rosseland mean free path l_R ,

$$\kappa_r = \frac{4}{3} c a_{SB} l_R T_r^3 = l_R \frac{4\pi^2}{45 \hbar^3 c^2} T_r^3 \stackrel{\text{D}}{=} 5484.0 l_R T_r^3, \quad (7.37)$$

where

$$l_R = l_R(\rho, T_e, T_r) = \frac{15}{4\pi^4} \int_0^{\infty} \frac{1}{\sigma_T n_e + \tilde{k}_a(\nu, \rho, T_e)} \frac{x^4 e^{-x}}{(1 - e^{-x})^2} dx, \quad x \equiv \frac{h\nu}{T_r}, \quad (7.38)$$

σ_T is the Thomson scattering cross-section, $\tilde{k}_a(\nu, \rho, T_e)$ [cm^{-1}] is the absorption coefficient of a photon $h\nu$ corrected for stimulated emission. If the values of l_R are provided from elsewhere as a function of one temperature only, $l_R = l_R(\rho, T)$, it is recommended to assign $l_R(\rho, T_e, T_r) = l_R(\rho, T_r)$. Analogously, the relaxation coefficient χ_{er} is defined as

$$\chi_{er}(\rho, T_e, T_r) = \frac{4\sigma_T}{m_e c} \frac{n_e}{\rho} a_{SB} T_r^4 + \frac{ca_{SB} T_e^4}{\rho(T_e - T_r)} \left[\frac{1}{l_P(\rho, T_e)} - \frac{15 h^4}{\pi^4 T_e^4} \int_0^\infty \tilde{k}_a(\nu, \rho, T_e) \frac{\nu^3 d\nu}{\exp(h\nu/T_r) - 1} \right], \quad (7.39)$$

where the Planckian mean free path $l_P(\rho, T_e)$ is given by

$$\frac{1}{l_P(\rho, T_e)} = \frac{15 h^4}{\pi^4 T_e^4} \int_0^\infty \tilde{k}_a(\nu, \rho, T_e) \frac{\nu^3 d\nu}{\exp(h\nu/T_e) - 1}. \quad (7.40)$$

Equations (7.39) and (7.40) imply that

$$\chi_{er}(\rho, T_e, 0) = \frac{\pi^2}{15 \hbar^3 c^2} \frac{T_e^3}{\rho l_P(\rho, T_e)} \stackrel{\text{D}}{=} 4113.0 \frac{T_e^3}{\rho l_P}. \quad (7.41)$$

If one wants to express $\chi_{er}(\rho, T_e, T_r)$ in terms of externally provided values of $l_P(\rho, T_e)$, one can, to a first approximation, assume $\chi_{er}(\rho, T_e, T_r) = \chi_{er}(\rho, T_e, 0)$.

Below we present simple analytical formulae for approximate evaluation of l_R and χ_{er} that have been adopted in the opacity model DEIRA-2. The more involved opacity model DEIRA-3 is described in Appendix B. The DEIRA-3 formulae describe the same physical processes but employ straightforward frequency integration instead of analytical approximations.

The present model describes radiation-matter interaction by taking into account the processes of Compton scattering, free-free absorption, and free-bound + bound-bound absorption. The free-free absorption (inverse bremsstrahlung) coefficient is calculated for a partially degenerate Fermi gas of free electrons. The contribution of the bound-bound and bound-free transitions is evaluated on the basis of the model proposed in Ref. [9]. In the DEIRA-2 version of the model the following approximate formulae are used:

$$l_R = \frac{1}{k_{cs} + k_{ff} + k_{ph}}, \quad (7.42)$$

$$\chi_{er} = \chi_{cs} + \chi_{ff} + \chi_{ph}. \quad (7.43)$$

Compton scattering:

$$k_{cs} \stackrel{\text{D}}{=} 0.04 \frac{\rho y Z_{mol}}{Z A_{mol}}, \quad \chi_{cs} \stackrel{\text{D}}{=} 0.94 \frac{y Z_{mol}}{Z A_{mol}} \varepsilon_r \stackrel{\text{D}}{=} 1.290 \frac{y Z_{mol}}{Z A_{mol}} T_r^4. \quad (7.44)$$

Inverse bremsstrahlung:

$$k_{ff} \stackrel{\text{D}}{=} \left(\frac{y}{Z}\right)^2 \frac{\rho \overline{Z^2}_{mol}}{A_{mol}} \frac{1}{T_r^2 \left[1 + 9.3 \theta_e^{3/2} (T_r/T_e)\right]}, \quad (7.45)$$

$$\chi_{ff} \stackrel{\text{D}}{=} 1.12 \times 10^5 \left(\frac{y}{Z}\right)^2 \frac{\overline{Z^2}_{mol}}{A_{mol}} \frac{T_e + T_r}{1 + 2.19 \theta_e^{3/2}}. \quad (7.46)$$

The quantity θ_e is defined in Eq. (7.34). Photoelectric absorption by hydrogen-like ions, $0 < Z - y \leq 1$:

$$k_{ph} \stackrel{\text{D}}{=} 1.2 (Z - y)_H \frac{\rho Z^4}{A T_r^3} \Phi_1(\omega_{r1}, -1.397), \quad (7.47)$$

$$\chi_{ph} \stackrel{\text{D}}{=} 759 \frac{Z^4}{A} (Z - y)_H \frac{T_e \Phi_2(\omega_{e1}, -1.397) - T_r \Phi_2(\omega_{r1}, -1.397)}{T_e - T_r}, \quad (7.48)$$

where

$$\omega_{e1} \stackrel{\text{D}}{=} \left(\frac{T_e}{0.0136 Z^2}\right)^2, \quad \omega_{r1} \stackrel{\text{D}}{=} \left(\frac{T_r}{0.0136 Z^2}\right)^2. \quad (7.49)$$

When y is close to Z , the equation-of-state data may lead to a large error in the small quantity $(Z - y)_H$. Hence, we use the following approximation in Eqs. (7.47) and (7.48)

$$(Z - y)_H \stackrel{\text{D}}{=} \left[1 + 0.665 \theta_e^{3/2} \exp \left(\frac{1}{\theta_e} - \frac{0.0136 Z^2}{T_e} \right) \right]^{-1}. \quad (7.50)$$

Photoelectric absorption by helium-like ions, $1 < Z - y \leq 2$:

$$k_{ph} \stackrel{\text{D}}{=} 1.2 \frac{\rho Z^4}{AT_r^3} [(2 + y - Z)\Phi_1(\omega_{r1}, -1.397) + 2(Z - y - 1)\Phi_1(\omega_{r2}, b_2)], \quad (7.51)$$

$$\begin{aligned} \chi_{ph} \stackrel{\text{D}}{=} 759 \frac{Z^4}{A} \left[(2 + y - Z) \frac{T_e \Phi_2(\omega_{e1}, -1.397) - T_r \Phi_2(\omega_{r1}, -1.397)}{T_e - T_r} + \right. \\ \left. + 2(Z - y - 1) \frac{T_e \Phi_2(\omega_{e2}, b_2) - T_r \Phi_2(\omega_{r2}, b_2)}{T_e - T_r} \right], \quad (7.52) \end{aligned}$$

where

$$\omega_{e2} \stackrel{\text{D}}{=} \left[\frac{T_e}{0.0136 (Z - 0.65)^2} \right]^2, \quad \omega_{r2} \stackrel{\text{D}}{=} \left[\frac{T_r}{0.0136 (Z - 0.65)^2} \right]^2, \quad (7.53)$$

$$b_2 \stackrel{\text{D}}{=} -1.397 + \frac{13.25}{(Z - 0.4)^2}. \quad (7.54)$$

Photoelectric absorption by lithium-like ions, $2 < Z - y \leq 3$:

$$k_{ph} \stackrel{\text{D}}{=} 2.4 \frac{\rho Z^4}{AT_r^3} [(3 + y - Z)\Phi_1(\omega_{r2}, b_2) + (Z - y - 2)\Phi_1(\omega_{r3}, b_3)], \quad (7.55)$$

$$\begin{aligned} \chi_{ph} \stackrel{\text{D}}{=} 1518.0 \frac{Z^4}{A} \left[(3 + y - Z) \frac{T_e \Phi_2(\omega_{e2}, b_2) - T_r \Phi_2(\omega_{r2}, b_2)}{T_e - T_r} + \right. \\ \left. + (Z - y - 2) \frac{T_e \Phi_2(\omega_{e3}, b_3) - T_r \Phi_2(\omega_{r3}, b_3)}{T_e - T_r} \right], \quad (7.56) \end{aligned}$$

where

$$\omega_{e3} \stackrel{\text{D}}{=} \left[\frac{T_e}{0.0036 (Z - 1.77)^2} \right]^2, \quad \omega_{r3} \stackrel{\text{D}}{=} \left[\frac{T_r}{0.0036 (Z - 1.77)^2} \right]^2, \quad (7.57)$$

$$b_3 \stackrel{\text{D}}{=} \frac{5.53}{(1 - 1.77/Z)^4} \ln \frac{11}{(1 - 1.77/Z)^4}. \quad (7.58)$$

Photoelectric absorption by higher ions, $3 < Z - y \leq Z$:

$$k_{ph} \stackrel{\text{D}}{=} 2.4 \frac{\rho Z^4}{AT_r^3} \Phi_1(\omega_{ry}, b_y), \quad (7.59)$$

$$\chi_{ph} \stackrel{\text{D}}{=} 1518.0 \frac{Z^4}{A} \frac{T_e \Phi_2(\omega_{ey}, b_y) - T_r \Phi_2(\omega_{ry}, b_y)}{T_e - T_r}, \quad (7.60)$$

where

$$\omega_{ey} = \left(\frac{T_e}{I_y} \right)^2, \quad \omega_{ry} = \left(\frac{T_r}{I_y} \right)^2, \quad (7.61)$$

$$b_y \stackrel{\text{D}}{=} \frac{0.245}{Z - y} \left(\frac{0.0272 Z^2}{I_y} \right)^2 \ln \left[\frac{1}{Z - y} \left(\frac{0.0272 Z^2}{I_y} \right)^2 \right]. \quad (7.62)$$

In the above formulae we used the functions

$$\Phi_1(\omega, b) = \frac{\omega}{210\omega + 5b + \frac{1}{4}(b+3)/\omega}, \quad (7.63)$$

$$\Phi_2(\omega, b) = \frac{\omega}{\omega + \frac{1}{2}(b+2.5)[1 + 1/(12\omega)]}. \quad (7.64)$$

The ionization potential of higher ions can be evaluated as

$$I_y \stackrel{D}{=} \begin{cases} 0.0063 (1+y)^{3/2} + 1.5 \times 10^{-7} (1+y)^4, & 10 < Z-y \leq Z, \\ 0.0036 (y+1.3)^2, & 2 < Z-y \leq 10, \\ 0.0136 (y+1.3)^2, & 0 < Z-y \leq 2. \end{cases} \quad (7.65)$$

7.3 Ion Heat Conduction and Viscosity

The limiting heat flux due to the ion heat conduction is defined as

$$F_{im} = f_{\kappa i} n_i \left(\frac{T_i}{m_i} \right)^{1/2} T_i \stackrel{D}{=} 29.97 f_{\kappa i} \rho \left(\frac{T_i}{A} \right)^{3/2}, \quad (7.66)$$

where $f_{\kappa i}$ is the flux limiting factor; regularly, $f_{\kappa i} = 0.5$ is assumed. Accordingly, the coefficient of the ion heat conduction corrected for the flux limit is defined as

$$\hat{\kappa}_i = \min \left\{ \kappa_i; \frac{F_{im}}{|\nabla T_i|} \right\}. \quad (7.67)$$

The transverse (with respect to the magnetic field) ion heat conduction coefficient is taken from Ref. [2]:

$$\kappa_i = \frac{n_i T_i}{m_i (\nu_{ii} + \nu_{ia})} \frac{2x_{ii}^2 + 2.645}{x_{ii}^4 + 2.70x_{ii}^2 + 0.677} \stackrel{D}{=} 93.89 \left(\frac{S_{mol} Z^2}{A_{mol} \sqrt{A}} \right) \frac{\rho T_i}{\nu_{ii} + \nu_{ia}} \frac{2x_{ii}^2 + 2.645}{x_{ii}^4 + 2.70x_{ii}^2 + 0.677}, \quad (7.68)$$

where

$$x_{ii} = \frac{eBy_*}{m_i c (\nu_{ii} + \nu_{ia})} \stackrel{D}{=} 964.9 \frac{By_*}{A(\nu_{ii} + \nu_{ia})}. \quad (7.69)$$

To the ion-ion collision frequency

$$\nu_{ii} = \frac{4\sqrt{\pi}}{3} \frac{e^4 n_i L_{ii}}{m_i^{1/2} T_i^{3/2}} \times \begin{cases} y, & y < 1, \\ y^4, & y \geq 1, \end{cases} \stackrel{D}{=} 9166.0 \frac{\rho \overline{Z^2}_{mol} L_{ii}}{Z^2 A_{mol} \sqrt{A} T_i^{3/2}} \times \begin{cases} y, & y < 1, \\ y^4, & y \geq 1, \end{cases} \quad (7.70)$$

we add the ion-atom collision frequency

$$\begin{aligned} \nu_{ia} &= \sigma_{ia} n_a \left(\frac{T_i}{m_i} \right)^{1/2} = \sigma_{ia} \frac{\rho}{m_i} \left(\frac{T_i}{m_i} \right)^{1/2} \times \begin{cases} (1-y), & y < 1, \\ 0, & y \geq 1, \end{cases} \stackrel{D}{=} \\ &\stackrel{D}{=} 1.871 \times 10^7 \frac{\rho T_i^{1/2}}{A^{3/2}} \times \begin{cases} (1-y), & y < 1, \\ 0, & y \geq 1, \end{cases} \end{aligned} \quad (7.71)$$

evaluated for the ion-atom scattering cross-section $\sigma_{ia} = 10^{-16} \text{ cm}^2$.

The two ion viscosity coefficients, η_0^i and η_1^i , that we need in our case, are taken from Ref. [2]:

$$\eta_0^i = \frac{0.96n_iT_i}{\nu_{ii} + \nu_{ia}} \stackrel{\text{D}}{=} 9.263 \frac{\rho T_i}{\bar{A}(\nu_{ii} + \nu_{ia})}, \quad (7.72)$$

$$\begin{aligned} \eta_1^i &= \frac{n_iT_i}{\nu_{ii} + \nu_{ia}} \frac{1.2(2x_{ii})^2 + 2.23}{(2x_{ii})^4 + 4.03(2x_{ii})^2 + 2.33} \stackrel{\text{D}}{=} \\ &\stackrel{\text{D}}{=} 9.649 \frac{\rho T_i}{\bar{A}(\nu_{ii} + \nu_{ia})} \frac{1.2(2x_{ii})^2 + 2.23}{(2x_{ii})^4 + 4.03(2x_{ii})^2 + 2.33}. \end{aligned} \quad (7.73)$$

The ion-ion Coulomb logarithm L_{ii} is calculated as

$$L_{ii} = \frac{1}{2} \ln(1 + \Lambda_{ii}^2), \quad (7.74)$$

where

$$\Lambda_{ii} = \frac{\frac{3}{2}T_i D_{ei}}{e^2 \left[y_*^4 + \frac{3}{4} \frac{m_e}{m_i} \left(\frac{\hbar^2 T_i}{m_e e^4} \right) \right]^{1/2}} \stackrel{\text{D}}{=} \frac{315.5T_i}{[D_{ei}^{-2}(y_*^4 + 1.512 \times 10^{-2}T_i/\bar{A})]^{1/2}}, \quad (7.75)$$

$$D_{ei}^{-2} \stackrel{\text{D}}{=} \frac{\rho y Z_{mol}}{Z A_{mol} T_F} + \left(\frac{y_*}{Z} \right)^2 \frac{\rho \bar{Z}^2_{mol}}{A_{mol} T_i} \times \begin{cases} y, & y < 1, \\ 1, & y \geq 1, \end{cases} \quad y_* = \begin{cases} 1, & y < 1, \\ y, & y \geq 1. \end{cases} \quad (7.76)$$

Functional form (7.75) has been chosen in agreement with the classical Coulomb scattering in the limit $\Lambda_{ii} \ll 1$; classical and quantum asymptotical formulae are matched in Eq. (7.75) by analogy with the electron-electron and electron-ion scattering [18].

7.4 Diffusion and Relaxation of the Energy of Fast Fusion Products

In this subsection we assume that the index (α) takes one of the three possible values, namely, α , $p3$, or $p14$. Each of the three sorts of fast charged fusion products is characterized by the set of constants listed in Table 3. Here, the principal quantity is the energy relaxation coefficient $\chi_{(\alpha)}$, defined such that $(\rho\chi_{(\alpha)})^{-1}$ is

Table 3: Constants for fast charged fusion products (in the DEIRA units).

(α)	α	$p3$	$p14$
$Z_{(\alpha)}$	2	1	1
$A_{(\alpha)}$	4	1	1
$v_{0(\alpha)}$	130.3	240.5	530.2
$c_{(\alpha)}$	0.077	0.12	0.13
$T_{(\alpha)}$	20	60	300

the decay time of the energy density $\mathcal{E}_{(\alpha)}$ [see Eqs (3.9)-(3.11)]. Its value does not depend on the presence of the magnetic field and can be split into two components,

$$\chi_{(\alpha)} = \chi_{(\alpha),n} + \chi_{(\alpha),c}, \quad (7.77)$$

representing, respectively, the loss of energy by nuclear scattering and by the Coulomb stopping. The contribution of nuclear scattering is important for the 14-MeV protons only, so that $\chi_{\alpha,n} = \chi_{p3,n} = 0$ in this DEIRA version.

The energy relaxation coefficient of the 14-MeV protons due to the nuclear scattering is given by [5]

$$\rho\chi_{p14,n} = v_{0p14} \sum_k \left\langle \frac{\Delta E}{E} \right\rangle_k \sigma_{nk} n_k, \quad (7.78)$$

where $v_{0p14} \stackrel{D}{=} 530.2$ is the birth velocity of 14-MeV protons,

$$\left\langle \frac{\Delta E}{E} \right\rangle_k = \frac{2A_k}{(1+A_k)^2} \langle 1 - \cos \theta \rangle_k \quad (7.79)$$

is the average relative energy loss of 14-MeV protons in a single act of elastic scattering off a nucleus with atomic mass A_k , σ_{nk} is the cross-section of such scattering, θ is the scattering angle in the center-of-mass system. To within the experimental errors, one can assume isotopic invariance of all the differential cross-sections — i.e. that 14-MeV protons are scattered exactly as 14-MeV neutrons, and there is no difference between the T and ^3He target nuclei. Also, for deuterium, we add up the non-elastic and elastic cross-sections to the total one. By using the experimental results for the total and differential cross-sections from Refs. [20, 21, 22, 23], we arrive at the values given in Table 4.

Table 4: Constants for nuclear scattering of 14-MeV protons and neutrons.

scatterer	p	D	T (^3He)
$\sigma_{nk,el}$ [barn]	0.69	0.61	0.98
$\sigma_{nk,tot}$ [barn]	0.69	0.80	0.98
$\langle 1 - \cos \theta \rangle$	1.0	0.70	0.70
$\sigma_{nk,tot} \left\langle \frac{\Delta E}{E} \right\rangle_k$ [barn]	0.35	0.25	0.26

From Table 4 one sees that, to a good accuracy, one can assume a universal value of the product $\sigma_{nk,tot} \left\langle \frac{\Delta E}{E} \right\rangle_k = 0.25$ barn for any D-T- ^3He fuel mixture, which yields

$$\chi_{p14,n} \stackrel{D}{=} 0.015 \frac{v_{0p14}}{A} = \frac{7.95}{A}. \quad (7.80)$$

The relaxation coefficient due to the Coulomb stopping can be calculated as [8]

$$\rho\chi_{(\alpha),c} = a_{(\alpha)} v_{0(\alpha)} (k_{e(\alpha)} + k_{i(\alpha)}), \quad (7.81)$$

where

$$a_{(\alpha)} = \frac{5}{2} - \frac{3}{2} \left[1 + \frac{2.4 \times 10^{-3}}{5 \times 10^{-4} + x_{e(\alpha)}^3} + c_{(\alpha)} x_{e(\alpha)}^3 \right]^{-1} \quad (7.82)$$

is a dimensionless coefficient determined by the dependence of the friction force acting on the decelerated particle on the energy of this particle, and

$$x_{e(\alpha)} = \left(\frac{m_e v_{0(\alpha)}^2}{2T_F} \right)^{1/2} \stackrel{D}{=} \frac{v_{0(\alpha)}}{187.5\sqrt{T_F}}; \quad (7.83)$$

the temperature T_F is defined in Eq. (7.33). The effective ‘‘absorption coefficient’’ $k_{(\alpha)}$ is defined as the ratio $F_{0(\alpha)}/E_{0(\alpha)}$, where $E_{0(\alpha)} = \frac{1}{2}m_A A_{(\alpha)} v_{0(\alpha)}^2$ is the initial energy of the corresponding fast particle, and $F_{0(\alpha)}$ is the initial value of the friction force decelerating this particle. In evaluating $F_{0(\alpha)}$, we can restrict ourselves to the stopping powers by the free plasma electrons and ions only (i.e. neglect the contribution of the bound

electrons) because, by the time fusion reactions become noticeable, both the fuel and the neighboring target shells are sufficiently highly ionized. As a result, we have [8]

$$\begin{aligned} v_{0(\alpha)}\rho^{-1}k_{e(\alpha)} &= \frac{4\pi e^4 Z_{(\alpha)}^2}{E_{0(\alpha)} v_{0(\alpha)}} \frac{n_e}{\rho m_e} \Phi(x_{e(\alpha)}) L_{e(\alpha)} \stackrel{\text{D}}{=} \\ &\stackrel{\text{D}}{=} \frac{yZ_{mol}}{ZA_{mol}} \left(\frac{1746}{v_{0(\alpha)}} \right)^3 \frac{Z_{(\alpha)}^2}{A_{(\alpha)}} \frac{x_{e(\alpha)}^3}{x_{e(\alpha)}^3 + 1.33} L_{e(\alpha)}, \end{aligned} \quad (7.84)$$

$$\begin{aligned} v_{0(\alpha)}\rho^{-1}k_{i(\alpha)} &= \frac{4\pi e^4 Z_{(\alpha)}^2}{E_{0(\alpha)} v_{0(\alpha)}} \frac{n_i}{\rho m_i} y^2 \left(1 + \frac{m_i}{m_{(\alpha)}} \right)^{1/2} L_{i(\alpha)} \stackrel{\text{D}}{=} \\ &\stackrel{\text{D}}{=} \left(\frac{yZ_{mol}}{ZA_{mol}} \right)^2 \left(\frac{143}{v_{0(\alpha)}} \right)^3 \frac{Z_{(\alpha)}^2}{A_{(\alpha)}} \left(1 + \frac{\bar{A}}{A_{(\alpha)}} \right)^{1/2} L_{i(\alpha)}. \end{aligned} \quad (7.85)$$

Here, the function $\Phi(x) = 2\pi^{-1/2} \left(\int_0^x e^{-t^2} dt - xe^{-x^2} \right)$ is approximated as $x^3/(x^3 + 1.33)$. For the Coulomb logarithms $L_{e(\alpha)}$ and $L_{i(\alpha)}$ we use the expressions from Ref. [4], reduced to the case of quantum scattering off the free electrons (but not the ions) and high projectile velocities $v_{0(\alpha)}$ compared to the thermal velocity $\sqrt{T_i/m_i}$ of the ions:

$$L_{e(\alpha)} = \ln \left[1 + \frac{\Lambda_{e(\alpha)}}{1 + 0.5 (\Lambda_{e(\alpha)})^{-1/2}} \right], \quad (7.86)$$

$$\Lambda_{e(\alpha)} = \frac{4T_F \eta_{(\alpha)}}{\hbar\omega_{pe}} \stackrel{\text{D}}{=} 139 T_F \eta_{(\alpha)} \left(\frac{ZA_{mol}}{\rho y Z_{mol}} \right)^{1/2}, \quad (7.87)$$

$$\begin{aligned} L_{i(\alpha)} &= \ln \left\{ \frac{2m_{(\alpha)}m_i}{m_{(\alpha)} + m_i} \frac{v_{0(\alpha)}\sqrt{2T_F\eta_{(\alpha)}/m_e}}{\hbar\omega_{pe} [1 + (1.781 y Z_{(\alpha)} e^2 / \hbar v_{0(\alpha)})^2]^{1/2}} \right\} \stackrel{\text{D}}{=} \\ &\stackrel{\text{D}}{=} 7.207 + \frac{1}{2} \ln \left[\left(\frac{\bar{A}}{1 + \bar{A}/A_{(\alpha)}} \right)^2 \frac{\bar{A}_e}{\rho y} \frac{T_F \eta_{(\alpha)} v_{0(\alpha)}^2}{1 + (39 y Z_{(\alpha)} / v_{0(\alpha)})^2} \right]. \end{aligned} \quad (7.88)$$

The effects of the Fermi degeneracy of the free electrons are accounted for by using T_F instead of T_e ; the function

$$\eta_{(\alpha)} = 0.353 + x_{e(\alpha)}^2 \frac{2.34 + x_{e(\alpha)}^3}{11 + x_{e(\alpha)}^3} \quad (7.89)$$

accounts for possible ‘‘subsonic’’ (with respect to the electron thermal speed) motion of the projectile at $v_{0(\alpha)} \lesssim \sqrt{T_F/m_e}$.

For alphas and 3-MeV protons, for which nuclear scattering is ignored, we can split the total energy dissipation $\chi_{(\alpha)}\mathcal{E}_{(\alpha)}$ between the electron and the ion plasma components by using a simple approximation (which introduces an error $\lesssim 20\%$)

$$\chi_{e(\alpha)} = \chi_{(\alpha)} f_{e(\alpha)}, \quad \chi_{i(\alpha)} = \chi_{(\alpha)} [1 - f_{e(\alpha)}], \quad (7.90)$$

$$f_{e(\alpha)} = \frac{T_{(\alpha)}}{T_{(\alpha)} + T_e}, \quad (7.91)$$

with the values of $T_{(\alpha)}$ from Table 3. For 14-MeV protons, we adopt the following two-term approximation

$$\begin{aligned} \chi_{ep14} &= \chi_{p14,n} f_{ep14,n} + \chi_{p14,c} \frac{T_{p14}}{T_{p14} + T_e}, \\ \chi_{ip14} &= \chi_{p14,n} (1 - f_{ep14,n}) + \chi_{p14,c} \left(1 - \frac{T_{p14}}{T_{p14} + T_e} \right), \end{aligned} \quad (7.92)$$

where $T_{p14} = 300$ keV, and $f_{ep14,n}$ is equal to the corresponding coefficient for 14-MeV neutrons given by Eq. (6.27), i.e.

$$f_{ep14,n} \stackrel{D}{=} [1 + (1 + \bar{A})^2 T_e / 750]^{-1}. \quad (7.93)$$

The diffusion coefficient $d_{(\alpha)}$ is affected (reduced) by the magnetic field. For Coulomb stopping, Liberman and Velikovich [7] have found that in the important particular case of $F_{(\alpha)} \propto E_{(\alpha)}^{1/2}$ one has

$$d_{(\alpha)} = \frac{v_{0(\alpha)}^2}{9 \rho \chi_{(\alpha)} + 4 \Omega_{(\alpha)}^2 / (\rho \chi_{(\alpha)})}, \quad (7.94)$$

where

$$\Omega_{(\alpha)} = \frac{e Z_{(\alpha)} B}{m_{(\alpha)} c} \stackrel{D}{=} 964.9 \frac{Z_{(\alpha)} B}{A_{(\alpha)}}. \quad (7.95)$$

Since in the non-magnetized plasma with $\Omega_{(\alpha)} = 0$ but in the general case of $-1 < \partial \ln F_{(\alpha)} / \partial \ln E_{(\alpha)} < \frac{1}{2}$ a more accurate formula will be [8]

$$d_{(\alpha)}|_{B=0} = \frac{v_{0(\alpha)}^2}{8 \rho \chi_{(\alpha)}}, \quad (7.96)$$

we adopt the following expression for the diffusion coefficient $d_{(\alpha)}$ of alphas and 3-MeV protons:

$$d_{(\alpha)} = \frac{v_{0(\alpha)}^2}{8 \rho \chi_{(\alpha)} + 4 \Omega_{(\alpha)}^2 / (\rho \chi_{(\alpha)})}. \quad (7.97)$$

For 14-MeV protons, for which nuclear scattering is also important, a more accurate formula will be

$$d_{p14} = \frac{v_{0p14}^2}{10 \rho \chi_{p14,n} + 8 \rho \chi_{p14,c} + 4 \Omega_{p14}^2 / [\rho (\chi_{p14,n} + \chi_{p14,c})]}. \quad (7.98)$$

8 FINITE DIFFERENCE SCHEME

8.1 Finite Difference Equations

We distinguish between the integer and half-integer numerical grid nodes. Integer nodes correspond to fixed values of the variable $m = m_j$, $j = 1, \dots, N + 1$ and discrete times $t = t_k$, $k = 1, 2, \dots$. Half-integer nodes correspond to $m = m_j + \frac{1}{2} \Delta m_j$, $t = t_k + \frac{1}{2} \Delta t_k$. The values of m , r , u , κ_e^* , κ_r^* , $\hat{\kappa}_e^*$, $\hat{\kappa}_r^*$, F_{em}^* , F_{rm}^* are assigned to integer nodes, the values of all the remaining variables — to half-integer nodes. Below, the indices j and k are omitted; the system of notation is illustrated in Fig. 1.

The finite difference scheme that we adopt for Eqs. (3.22)–(3.34) is as follows:

$$\frac{\bar{r} - r}{\Delta t} = \frac{1}{2}(u + \bar{u}), \quad (8.1)$$

$$\frac{\bar{u} - u}{\Delta t} + 2 \bar{r}^s \frac{P - P_-}{\Delta m + \Delta m_-} = \frac{2}{\bar{r}} \frac{\eta_{ten} \Sigma - \eta_{ten-} \Sigma_-}{\Delta m + \Delta m_-}, \quad (8.2)$$

$$\begin{aligned} \epsilon_{eT} \frac{\bar{T}_e - T_e}{\Delta t} = & \frac{1}{\Delta m} \left[\bar{r}^s \frac{2 \hat{\kappa}_e^*}{\bar{r}_+ - \bar{r}_-} (\bar{T}_{e-} - \bar{T}_e) - \bar{r}_+^s \frac{2 \hat{\kappa}_{e+}^*}{\bar{r}_{+2} - \bar{r}} (\bar{T}_e - \bar{T}_{e+}) \right] - \\ & - \chi_{ei} (\bar{T}_e - \bar{T}_i) - \chi_{er} (\bar{T}_e - \bar{T}_r) + Q_e, \end{aligned} \quad (8.3)$$

$$\epsilon_{iT} \frac{\bar{T}_i - T_i}{\Delta t} = \frac{1}{\Delta m} \left[\bar{r}^s \frac{2 \hat{\kappa}_i^*}{\bar{r}_+ - \bar{r}_-} (\bar{T}_{i-} - \bar{T}_i) - \bar{r}_+^s \frac{2 \hat{\kappa}_{i+}^*}{\bar{r}_{+2} - \bar{r}} (\bar{T}_i - \bar{T}_{i+}) \right] + \chi_{ei} (\bar{T}_e - \bar{T}_i) + Q_i, \quad (8.4)$$

$$\begin{aligned} 4 a_{SB} T_r^3 \bar{V} \frac{\bar{T}_r - T_r}{\Delta t} + a_{SB} T_r^4 \left(\frac{\bar{V} - V}{\Delta t} + \frac{1}{3} \dot{V} \right) = & \chi_{er} (\bar{T}_e - \bar{T}_r) + \\ & + \frac{1}{\Delta m} \left[\bar{r}^s \frac{2 \hat{\kappa}_r^*}{\bar{r}_+ - \bar{r}_-} (\bar{T}_{r-} - \bar{T}_r) - \bar{r}_+^s \frac{2 \hat{\kappa}_{r+}^*}{\bar{r}_{+2} - \bar{r}} (\bar{T}_r - \bar{T}_{r+}) \right], \end{aligned} \quad (8.5)$$

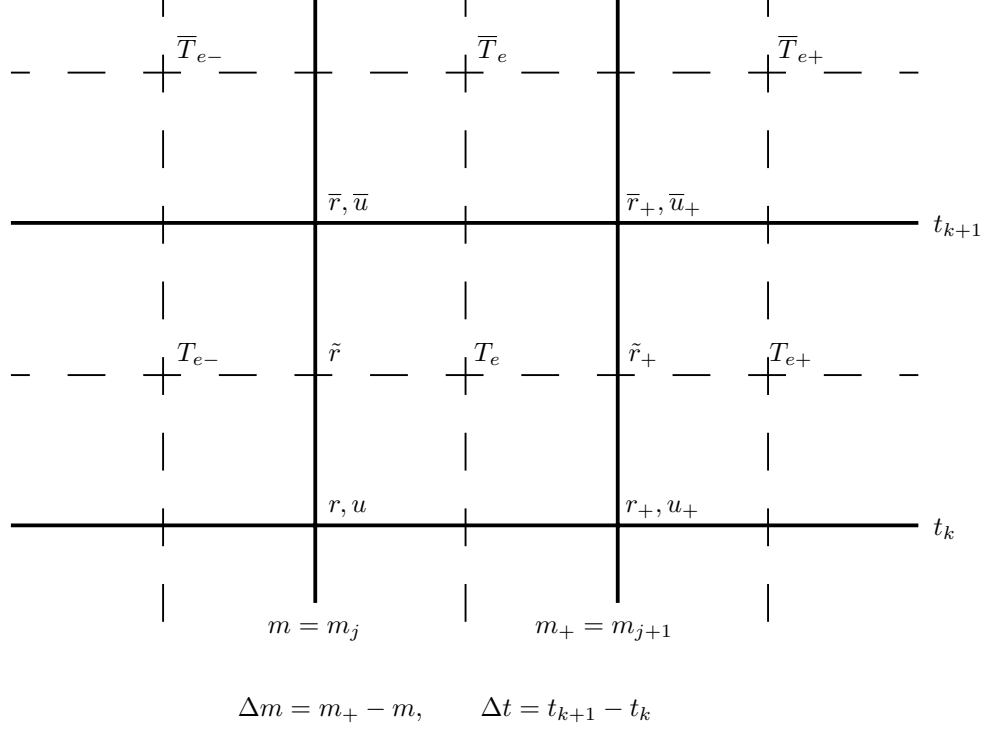


Figure 1: Numerical grid.

$$\frac{\bar{B}\bar{V} - BV}{\Delta t} = \frac{1}{\Delta m} \left[\bar{r}^s \frac{c^2}{4\pi} \frac{\eta_{\perp-} + \eta_{\perp}}{\bar{r}_+ - \bar{r}_-} (\bar{B}_- - \bar{B}) - \bar{r}_+^s \frac{c^2}{4\pi} \frac{\eta_{\perp} + \eta_{\perp+}}{\bar{r}_{+2} - \bar{r}} (\bar{B} - \bar{B}_+) \right], \quad (8.6)$$

$$\begin{aligned} \frac{\bar{V}\bar{\mathcal{E}}_{(\alpha)} - V\mathcal{E}_{(\alpha)}}{\Delta t} + \frac{2}{3}\mathcal{E}_{(\alpha)}\dot{V} + \chi_{(\alpha)}\bar{\mathcal{E}}_{(\alpha)} &= Q_{(\alpha)} + \\ &+ \frac{1}{\Delta m} \left[\bar{r}^s \frac{d_{(\alpha)-} + d_{(\alpha)}}{\bar{r}_+ - \bar{r}_-} (\bar{\mathcal{E}}_{(\alpha)-} - \bar{\mathcal{E}}_{(\alpha)}) - \bar{r}_+^s \frac{d_{(\alpha)} + d_{(\alpha)+}}{\bar{r}_{+2} - \bar{r}} (\bar{\mathcal{E}}_{(\alpha)} - \bar{\mathcal{E}}_{(\alpha)+}) \right], \end{aligned} \quad (8.7)$$

$$\frac{\bar{X}_D - X_D}{\tau} = -\bar{X}_T q_{DT} - 2X_D q_{DD} - \bar{X}_{He} q_{DHe}, \quad (8.8)$$

$$\bar{X}_T = \frac{X_T + \frac{1}{2}\tau X_D q_{DD}}{1 + \tau q_{DT}}, \quad (8.9)$$

$$\bar{X}_{He} = \frac{X_{He} + \frac{1}{2}\tau X_D q_{DD}}{1 + \tau q_{DHe}}, \quad (8.10)$$

$$\begin{cases} \bar{X}_B = \frac{X_B}{1 + \tau_{BH} X_H}, & \bar{X}_H = \bar{X}_B + X_H - X_B, & \text{when } X_B < X_H, \\ \bar{X}_H = \frac{X_H}{1 + \tau_{BH} X_B}, & \bar{X}_B = \bar{X}_H + X_B - X_H, & \text{when } X_B > X_H. \end{cases} \quad (8.11)$$

In Eq. (8.7) index (α) runs through the values α , $p3$, and $p14$. In the above equations we introduced the following quantities:

$$\tilde{r} = r + \frac{1}{2}u \Delta t, \quad (8.12)$$

$$\Delta m = m_+ - m, \quad (8.13)$$

$$P = -\eta_{sca} \dot{V} + P_e + P_i + \frac{B^2}{8\pi} + \frac{1}{3} a_{SB} T_r^4 + \frac{2}{3} (\mathcal{E}_\alpha + \mathcal{E}_{p3} + \mathcal{E}_{p14}), \quad (8.14)$$

$$\dot{V} = \frac{(u_+ + \bar{u}_+) \tilde{r}_+^s - (u + \bar{u}) \tilde{r}^s}{2 \Delta m}, \quad (8.15)$$

$$\Sigma = \frac{1}{2 \Delta m} \left[\frac{u_+ + \bar{u}_+}{\tilde{r}_+} - \frac{u + \bar{u}}{\tilde{r}} \right], \quad (8.16)$$

$$\epsilon_{eT} \equiv \frac{\partial \epsilon_e}{\partial T_e}, \quad \epsilon_{iT} \equiv \frac{\partial \epsilon_i}{\partial T_i}, \quad \epsilon_{eV} \equiv \frac{\partial \epsilon_e}{\partial V}, \quad \epsilon_{iV} \equiv \frac{\partial \epsilon_i}{\partial V}, \quad (8.17)$$

$$Q_e = Q_B + Q_{dr} + Q_{ecl} + Q_{en} + \chi_{e\alpha} \bar{\mathcal{E}}_\alpha + \chi_{ep3} \bar{\mathcal{E}}_{p3} + \chi_{ep14} \bar{\mathcal{E}}_{p14} - (P_e + \epsilon_{eV}) \dot{V}, \quad (8.18)$$

$$Q_i = Q_{icl} + Q_{in} + \chi_{i\alpha} \bar{\mathcal{E}}_\alpha + \chi_{ip3} \bar{\mathcal{E}}_{p3} + \chi_{ip14} \bar{\mathcal{E}}_{p14} - (P_i + \epsilon_{iV}) \dot{V} + \\ + \eta_{sca} (\dot{V})^2 + \eta_{ten} (\Sigma)^2, \quad (8.19)$$

$$Q_B = \bar{r}^s \frac{1}{2} \left(\frac{c}{4\pi} \right)^2 (\eta_{\perp-} + \eta_{\perp}) \left(\frac{\bar{B}_- - \bar{B}}{\bar{r}_+ - \bar{r}_-} \right) \left(\frac{\tilde{B}_- - \tilde{B}}{\Delta m} \right) + \\ + \bar{r}_+^s \frac{1}{2} \left(\frac{c}{4\pi} \right)^2 (\eta_{\perp} + \eta_{\perp+}) \left(\frac{\bar{B} - \bar{B}_+}{\bar{r}_{+2} - \bar{r}} \right) \left(\frac{\tilde{B} - \tilde{B}_+}{\Delta m} \right), \quad \tilde{B} = \frac{1}{2}(B + \bar{B}), \quad (8.20)$$

$$\tau = \Delta t \frac{X_D}{V A_{mol}}, \quad \tau_{BH} = \frac{\Delta t}{V A_{mol}} q_{BH}. \quad (8.21)$$

Coefficients κ_e^* , $\hat{\kappa}_e^*$, κ_i^* , $\hat{\kappa}_i^*$, κ_r^* , $\hat{\kappa}_r^*$ are defined at the integer nodes of numerical grid, i.e. at the boundaries between grid intervals. They are evaluated according to the following formulae:

$$\hat{\kappa}_e^* = \min \left[\kappa_e^*; \quad F_{em}^* \frac{0.5(r_+ - r_-)}{|T_e - T_{e-}|} \right], \quad (8.22)$$

$$\hat{\kappa}_i^* = \min \left[\kappa_i^*; \quad F_{im}^* \frac{0.5(r_+ - r_-)}{|T_i - T_{i-}|} \right], \quad (8.23)$$

$$\hat{\kappa}_r^* = \min \left[\kappa_r^*; \quad F_{rm}^* \frac{0.5(r_+ - r_-)}{|T_r - T_{r-}|} \right], \quad (8.24)$$

$$\kappa_e^* = 0.5(\kappa_{e-} + \kappa_e), \quad F_{em}^* = \begin{cases} F_{em-}, & T_{e-} \geq T_e, \\ F_{em}, & T_{e-} < T_e, \end{cases} \quad (8.25)$$

$$\kappa_i^* = 0.5(\kappa_{i-} + \kappa_i), \quad F_{im}^* = \begin{cases} F_{im-}, & T_{i-} \geq T_i, \\ F_{im}, & T_{i-} < T_i, \end{cases} \quad (8.26)$$

$$\kappa_r^* = 0.5(\kappa_{r-} + \kappa_r), \quad F_{rm}^* = \begin{cases} F_{rm-}, & T_{r-} \geq T_r, \\ F_{rm}, & T_{r-} < T_r. \end{cases} \quad (8.27)$$

The quantities F_{em} , F_{im} , and F_{rm} are defined in Eqs. (7.1), (7.66), and (7.36). The new values of the specific volume are calculated from the formula

$$\bar{V} = \frac{(\bar{r}_+ + \frac{1}{2} \bar{u}_+ \Delta t)^{s+1} - (\bar{r} + \frac{1}{2} \bar{u} \Delta t)^{s+1}}{(s+1) \Delta m}, \quad (8.28)$$

which implies rigorous conservation of mass in each mesh interval Δm .

For the coefficients of the total viscosity η_{sca} and η_{ten} the following expressions are used

$$\eta_{sca} = \frac{\eta_{i,sc}}{V} + \begin{cases} 0, & u_+ \geq u, \\ \frac{\Delta m}{V \langle \tilde{r}^s \rangle} [\mu_{1av,sc} u_s + \mu_{2av,sc} (u - u_+)], & u_+ < u, \end{cases} \quad (8.29)$$

$$\eta_{ten} = \frac{\eta_{i,tn}}{V} \langle \tilde{r}^{2s+2} \rangle + \begin{cases} 0, & u_+ \geq u, \\ \frac{\Delta m \langle \tilde{r}^{s+2} \rangle}{V} [\mu_{1av,tn} u_s + \mu_{2av,tn} (u - u_+)], & u_+ < u, \end{cases} \quad (8.30)$$

where

$$\langle \tilde{r}^s \rangle = (1 - \sigma_{av,sc}) \tilde{r}^s + \sigma_{av,sc} \tilde{r}_+^s, \quad (8.31)$$

$$\langle \tilde{r}^{s+2} \rangle = (1 - \sigma_{av,tn}) \tilde{r}^{s+2} + \sigma_{av,tn} \tilde{r}_+^{s+2}, \quad (8.32)$$

$$\langle \tilde{r}^{2s+2} \rangle = (1 - \sigma_{av,tn}) \tilde{r}^{2s+2} + \sigma_{av,tn} \tilde{r}_+^{2s+2}, \quad (8.33)$$

u_s is the adiabatic sound velocity defined in Eq. (5.10). In each of the Eqs. (8.29) and (8.30), the first and the second terms on the right-hand side represent, respectively, the physical and the artificial components of the viscosity. From Eqs. (8.29)–(8.32) it is seen that the adopted version of the artificial viscosity contains six dimensionless parameters: $\mu_{1av,sc}$ – the coefficient of linear scalar viscosity, $\mu_{2av,sc}$ – the coefficient of quadratic scalar viscosity (the Neumann-Richtmyer viscosity), $\mu_{1av,tn}$ – the coefficient of linear “tensor” viscosity, $\mu_{2av,tn}$ – the coefficient of quadratic “tensor” viscosity, and $0 < \sigma_{av,sc} \leq 1$ and $0 \leq \sigma_{av,tn} \leq 1$ – two free parameters of the approximation. The choice of specific values for these 6 parameters is discussed in Ref. [3]. A recommended set of values for the “center” and “closed cavity” left boundary conditions is given in Table 5. In the case of the “open halfspace” left boundary, when the artificial t-viscosity is turned off, one has to assign a non-zero value of $\mu_{2av,sc}$ (say, $\mu_{2av,sc} = 2$).

Table 5: Recommended values of the 6 parameters for artificial viscosity when IFLBND = 0,1

$\mu_{1av,sc}$	$\mu_{2av,sc}$	$\sigma_{av,sc}$	$\mu_{1av,tn}$	$\mu_{2av,tn}$	$\sigma_{av,tn}$
0.1	0	1	0	2	0.1

8.2 Conservation Laws

The finite difference equations (8.1)–(8.10) ought to be augmented by the finite difference expressions for the momentum and various energy components. Omitting for simplicity the trivial factor $K(s)$ given by Eq. (3.18), we adopt the following expressions for the electron, ion, radiative, magnetic, and fast-product components of the internal energy content in a Lagrangean mesh interval Δm (assigned to half-integer nodes of the grid):

$$\begin{aligned} \Delta E_e &= \epsilon_e \Delta m, & \Delta E_i &= \epsilon_i \Delta m, & \Delta E_r &= a_{SB} T_r^4 V \Delta m, \\ \Delta E_B &= \frac{1}{8\pi} B^2 V \Delta m, & \Delta E_{(\alpha)} &= \mathcal{E}_{(\alpha)} V \Delta m. \end{aligned} \quad (8.34)$$

The momentum and kinetic energy are naturally assigned to integer rather than half-integer grid nodes — together with the velocities u . In doing so, we assume — in compliance with Eq. (8.2) — that each integer node has a mass equal to the arithmetic mean of the masses of the two adjacent mesh intervals. The momentum and kinetic energy of a mass interval (assigned to a half-integer node) is defined as the arithmetic

mean of the momenta and kinetic energies of the corresponding left and right integer nodes:

$$\Delta p = \begin{cases} \frac{1}{2}\Delta m_1 u_1 + \frac{1}{4}(\Delta m_1 + \Delta m_2)u_2, & j = 1, \\ \frac{1}{4}[(\Delta m_- + \Delta m)u + (\Delta m + \Delta m_+)u_+], & j = 2, \dots, N-1, \\ \frac{1}{4}(\Delta m_{N-1} + \Delta m_N)u_N + \frac{1}{2}\Delta m_N u_{N+1}, & j = N; \end{cases} \quad (8.35)$$

$$\Delta E_{kin} = \begin{cases} \frac{1}{4}\Delta m_1 u_1^2 + \frac{1}{8}(\Delta m_1 + \Delta m_2)u_2^2, & j = 1, \\ \frac{1}{8}[(\Delta m_- + \Delta m)u^2 + (\Delta m + \Delta m_+)u_+^2], & j = 2, \dots, N-1, \\ \frac{1}{8}(\Delta m_{N-1} + \Delta m_N)u_N^2 + \frac{1}{4}\Delta m_N u_{N+1}^2, & j = N. \end{cases} \quad (8.36)$$

Next, define the momentum flux density

$$\Pi = \begin{cases} \frac{1}{2}(P_{bl} - P_1), & j = 1, \\ \frac{1}{2}\left[\tilde{r}^s(P_- - P) - \frac{1}{\tilde{r}}(\eta_{ten-\Sigma_-} - \eta_{ten\Sigma})\right], & j = 2, \dots, N, \\ \frac{1}{2}\left[\tilde{r}_{N+1}^s(P_N - P_{br}) - \frac{1}{\tilde{r}_{N+1}}\eta_{ten,N}\Sigma_N\right], & j = N+1, \end{cases} \quad (8.37)$$

the flux density of the internal energy (work by pressure forces)

$$\mathcal{F}_{kin} = \begin{cases} \frac{1}{2}(u_1 + \bar{u}_1)P_{bl}, & j = 1, \\ \frac{1}{4}(u + \bar{u})\left[\tilde{r}^s(P_- + P) - \frac{1}{\tilde{r}}(\eta_{ten-\Sigma_-} + \eta_{ten\Sigma})\right], & j = 2, \dots, N, \\ \frac{1}{2}(u_{N+1} + \bar{u}_{N+1})\tilde{r}_{N+1}^s P_{br}, & j = N+1, \end{cases} \quad (8.38)$$

the electron, ion, and radiation heat flux densities

$$\mathcal{F}_e = \begin{cases} 0, & j = 1, \\ \tilde{r}^s \frac{2\hat{\kappa}_e^*}{\tilde{r}_+ - \tilde{r}_-} (\bar{T}_{e-} - \bar{T}_e), & j = 2, \dots, N, \\ 0, & j = N+1, \end{cases} \quad (8.39)$$

$$\mathcal{F}_i = \begin{cases} 0, & j = 1, \\ \tilde{r}^s \frac{2\hat{\kappa}_i^*}{\tilde{r}_+ - \tilde{r}_-} (\bar{T}_{i-} - \bar{T}_i), & j = 2, \dots, N, \\ 0, & j = N+1, \end{cases} \quad (8.40)$$

$$\mathcal{F}_r = \begin{cases} 0, & j = 1 \wedge \text{IFLBN} = 0, 1, \\ \frac{1}{4}ca_{SB}(T_{rlex}^4 - T_{r,1}^3 \bar{T}_{r,1}), & j = 1 \wedge \text{IFLBN} = -1, \\ \tilde{r}^s \frac{2\hat{\kappa}_r^*}{\tilde{r}_+ - \tilde{r}_-} (\bar{T}_{r-} - \bar{T}_r), & j = 2, \dots, N, \\ \frac{1}{4}ca_{SB}\tilde{r}_{N+1}^s (T_{r,N}^3 \bar{T}_{r,N} - T_{r,ex}^4), & j = N+1, \end{cases} \quad (8.41)$$

and the flux densities of the energy of fast fusion products

$$\mathcal{F}_{(\alpha)} = \begin{cases} 0, & j = 1 \wedge \text{IFLBND} = 0, 1, \\ -\frac{2d_{(\alpha),1}}{\bar{r}_2 - \bar{r}_1} \bar{\mathcal{E}}_{(\alpha),1}, & j = 1 \wedge \text{IFLBND} = -1, \\ \bar{r}^s \frac{d_{(\alpha)-} + d_{(\alpha)}}{\bar{r}_+ - \bar{r}_-} (\bar{\mathcal{E}}_{(\alpha)-} - \bar{\mathcal{E}}_{(\alpha)}), & j = 2, \dots, N, \\ \bar{r}_{N+1}^s \frac{2d_{(\alpha),N}}{\bar{r}_{N+1} - \bar{r}_N} \bar{\mathcal{E}}_{(\alpha),N}, & j = N + 1. \end{cases} \quad (8.42)$$

across the left boundary of the j -th mesh interval (j -th integer node of the grid). Expressions (8.38)–(8.42) for the flux densities account for the boundary conditions (4.1)–(4.15).

Having adopted the above discretized definitions of the momentum, energy, and fluxes, one readily ascertains that the numerical scheme (8.1)–(8.11) has the following conservative properties. First of all, when just the equations of hydrodynamics are considered separately, the numerical scheme (8.1)–(8.4), (8.28) is fully conservative provided that $\epsilon_{eT} = \text{constant}$, $\epsilon_{iT} = \text{constant}$, and $\epsilon_{eV} = \epsilon_{iV} = 0$ because the increments of the momentum Δp and the total energy $\Delta E = \Delta E_{kin} + \Delta E_e + \Delta E_i$ in any mesh interval for any time step can be cast in the divergent form

$$\frac{\overline{\Delta p} - \Delta p}{\Delta t} = \Pi + \Pi_+, \quad (8.43)$$

$$\frac{\overline{\Delta E} - \Delta E}{\Delta t} = \mathcal{F}_{kin} - \mathcal{F}_{kin+} + \mathcal{F}_e - \mathcal{F}_{e+} + \mathcal{F}_i - \mathcal{F}_{i+} + Q_{cl} + Q_n + Q_{dr}. \quad (8.44)$$

Moreover, the total energy $\Delta E = \Delta E_{kin} + \Delta E_e + \Delta E_i + \Delta E_\alpha + \Delta E_{p3} + \Delta E_{p14}$ is still conserved when the diffusion equations (8.7) for the energy density of fast fusion products are added to the hydrodynamic equations (8.1)–(8.4) (because expressions (8.18) and (8.19) for Q_e and Q_i contain “new” values $\bar{\mathcal{E}}_\alpha$, $\bar{\mathcal{E}}_{p3}$, and $\bar{\mathcal{E}}_{p14}$). The conservation of energy is violated, however, by the radiation diffusion equation (8.5) because the heat capacity of radiation $4a_{SB}T_r$ is strongly temperature dependent and taken from the previous time step.

A special attention should be paid to the magnetic energy ΔE_B . From Eq. (3.27) one derives the following equation for the specific (per unit mass) density $B^2V/8\pi$ of the magnetic energy:

$$\frac{\partial}{\partial t} \left(\frac{B^2V}{8\pi} \right) + \frac{B^2}{8\pi} \frac{\partial V}{\partial t} = \frac{\partial}{\partial m} \left[\left(\frac{c}{4\pi} \right)^2 r^s \eta_\perp B \frac{\partial B}{\partial r} \right] - \left(\frac{c}{4\pi} \right)^2 \eta_\perp V \left(\frac{\partial B}{\partial r} \right)^2. \quad (8.45)$$

The second term on the right-hand side of Eq. (8.45) is the Joule heating. For our numerical scheme to be conservative with respect to the magnetic energy ΔE_B , the discretized form of Eq. (8.45) should look like

$$\frac{1}{8\pi} \frac{\overline{B^2V} - B^2V}{\Delta t} + \frac{B^2}{8\pi} \dot{V} = \frac{1}{\Delta m} (\mathcal{F}_B - \mathcal{F}_{B+}) - Q_B, \quad (8.46)$$

where \mathcal{F}_B and Q_B are the finite-difference approximations of the diffusion flux and Joule heating,

$$\mathcal{F}_B \approx \left(\frac{c}{4\pi} \right)^2 r^s \eta_\perp B \frac{\partial B}{\partial r}, \quad Q_B \approx \left(\frac{c}{4\pi} \right)^2 \eta_\perp V \left(\frac{\partial B}{\partial r} \right)^2. \quad (8.47)$$

When we multiply Eq. (8.6) by

$$\frac{1}{4\pi} \tilde{B} \equiv \frac{1}{8\pi} (B + \bar{B}) \quad (8.48)$$

we obtain

$$\begin{aligned} \frac{1}{8\pi} \frac{\overline{B^2V} - B^2V}{\Delta t} + \left(\frac{B\bar{B}}{8\pi} \right) \frac{\bar{V} - V}{\Delta t} &= \frac{1}{\Delta m} \left(\frac{c}{4\pi} \right)^2 \left[\bar{r}^s \frac{\eta_{\perp-} + \eta_{\perp}}{\bar{r}_+ - \bar{r}_-} (\bar{B}_- - \bar{B}) \tilde{B}_- \right. \\ &\quad \left. - \bar{r}_+^s \frac{\eta_{\perp} + \eta_{\perp+}}{\bar{r}_{+2} - \bar{r}} (\bar{B} - \bar{B}_+) \tilde{B} \right]. \end{aligned} \quad (8.49)$$

Although the term $\left(\frac{B\bar{B}}{8\pi}\right)\frac{\bar{V}-V}{\Delta t}$ is not exactly $\frac{B^2}{8\pi}\dot{V}$, it approaches $\frac{B^2}{8\pi}\dot{V}$ in the limit of $\Delta t \rightarrow 0$ (or at $u \rightarrow 0, \bar{u} \rightarrow 0$). Finally, we can rewrite Eq. (8.49) in the form

$$\begin{aligned} \frac{1}{8\pi}\frac{\bar{B}^2\bar{V}-B^2V}{\Delta t} + \left(\frac{B\bar{B}}{8\pi}\right)\frac{\bar{V}-V}{\Delta t} &= \frac{1}{\Delta m}\left(\frac{c}{4\pi}\right)^2 \left[\bar{r}^s \frac{\eta_{\perp-} + \eta_{\perp}}{\bar{r}_+ - \bar{r}_-} \frac{\tilde{B}_- + \tilde{B}}{2} (\bar{B}_- - \bar{B}) - \right. \\ &\quad \left. - \bar{r}_+^s \frac{\eta_{\perp} + \eta_{\perp+}}{\bar{r}_{+2} - \bar{r}} \frac{\tilde{B} + \tilde{B}_+}{2} (\bar{B} - \bar{B}_+) \right] - \\ &\quad - \left(\frac{c}{4\pi}\right)^2 \frac{1}{2\Delta m} \left[\bar{r}^s \frac{\eta_{\perp-} + \eta_{\perp}}{\bar{r}_+ - \bar{r}_-} (\bar{B} - \bar{B}_-) (\tilde{B} - \tilde{B}_-) + \bar{r}_+^s \frac{\eta_{\perp} + \eta_{\perp+}}{\bar{r}_{+2} - \bar{r}} (\bar{B}_+ - \bar{B}) (\tilde{B}_+ - \tilde{B}) \right], \end{aligned} \quad (8.50)$$

which implies expression (8.20) for the Joule heating Q_B and the following expression for the flux density \mathcal{F}_B of the magnetic energy,

$$\mathcal{F}_B = \frac{1}{2} \left(\frac{c}{4\pi}\right)^2 \bar{r}^s (\eta_{\perp-} + \eta_{\perp}) (\tilde{B}_- + \tilde{B}) \frac{\bar{B}_- - \bar{B}}{\bar{r}_+ - \bar{r}_-}. \quad (8.51)$$

The finite difference approximation to the artificial viscosity is constructed in such a way that the viscous dissipation of the kinetic energy is strictly non-negative and heats up only the ion plasma component [see Eq. (8.19)]. However, the increment of the specific entropy may, strictly speaking, sometimes be negative because Eqs (8.3) and (8.4) are written for the internal energy rather than the specific entropy and contain the “old” value of pressure P . The entropy disbalance decreases in direct proportion with the value of the time step Δt . Note also that, since the equation of motion (8.2) contains the “old” pressure P , our numerical scheme is an explicit one and is subject to the Courant restriction on the values of the time step Δt .

All the relaxation and diffusion terms in Eqs (8.3)–(8.7) use the “new” values of the corresponding principal variables $\bar{T}_e, \dots, \bar{\mathcal{E}}_\alpha, \dots$. This removes the problem of numerical stability with respect to these processes but does not imply that these processes do not impose any additional restrictions on the values of Δt : such restrictions may be dictated by strong dependence of the corresponding diffusion and relaxation coefficients on dynamic variables when the values of the coefficients are taken from the previous time step.

The numerical scheme for the equations of nuclear kinetics (8.8)–(8.10) is chosen in such a form that it admits large relative changes in the concentrations of tritium, X_T , and helium-3, X_{He} , (but not in the concentration of deuterium X_D) in one time step. The initial values of X_T and X_{He} can be arbitrarily small, while the initial value of X_D should always be on the order of unity.

9 NUMERICAL ALGORITHM

Once the “old” values r, u, T_e, \dots of all the principal variables are known, the thermodynamic functions and the kinetic coefficients have been calculated, and the value of the next time step Δt is specified, one can solve the finite difference equations (8.1)–(8.10) to calculate the “new” values of the principal dependent variables $\bar{r}, \bar{u}, \bar{T}_e, \dots$. This step is realized in the subroutine UPSLOI, and the scheme of solution of Eqs. (8.1)–(8.10) described below is in fact a block-scheme of this subroutine. The subroutine UPSLOI consists of 5 major blocks (NEWXDT, NEWRU, NEWREAL, NEWHZ, NEWTTT), each of which solves a certain subgroup of equations (8.1)–(8.11).

I. Block NEWXDT. In this block, new concentrations $\bar{X}_T, \bar{X}_{He}, \bar{X}_D, \bar{X}_B,$ and \bar{X}_H are calculated from Eqs (8.8)–(8.11).

II. Block NEWRU. In this block, equations (8.1) and (8.2) are solved and the values of $\bar{r}, \bar{u},$ and \bar{V} are calculated. The solution is obtained through the following steps.

1) From Eq. (8.12) the radii at half-step \tilde{r} are calculated.

2) The values of \bar{u} are calculated by solving the system of linear equations (8.2). The scheme of solution is as follows. First of all, we introduce a representation

$$\bar{u} = A\bar{u}_+ + B, \quad (9.1)$$

where A and B (not to be mixed up with the magnetic field strength B) are arrays of unknown coefficients. Since the general form of Eq. (8.2) is

$$\alpha\bar{u}_- + \beta\bar{u} + \gamma\bar{u}_+ + \delta = 0, \quad (9.2)$$

where α, β, γ , and δ are known, we substitute into it the expression $\bar{u}_- = A_- \bar{u} + B_-$ and obtain the following recurrent formulae for calculating the arrays A and B :

$$A = \mathcal{T} \left[\eta_s \tilde{r}_+^s + \eta_t \left(\frac{\tilde{r}_+}{\tilde{r}} \right)^{s+1} \right] / \Omega, \quad (9.3)$$

$$B = \left\{ u + \mathcal{T} \left[2(P_{nv-} - P_{nv}) + \eta_s (u_+ \tilde{r}_+^s - u \tilde{r}^s) - \eta_{s-} (u \tilde{r}^s - u_- \tilde{r}_-^s - B_- \tilde{r}_-^s) + \eta_t \left(\frac{\tilde{r}_+}{\tilde{r}} \right)^{s+2} \left(u_+ \frac{\tilde{r}}{\tilde{r}_+} - u \right) - \eta_{t-} \left(u - (u_- + B_-) \frac{\tilde{r}}{\tilde{r}_-} \right) \right] \right\} / \Omega, \quad (9.4)$$

$$\Omega = 1 + \mathcal{T} \left[\eta_s \tilde{r}^s + \eta_{s-} (\tilde{r}^s - A_- \tilde{r}_-^s) + \eta_t \left(\frac{\tilde{r}_+}{\tilde{r}} \right)^{s+2} + \eta_{t-} \left(1 - A_- \frac{\tilde{r}}{\tilde{r}_-} \right) \right], \quad (9.5)$$

where

$$\eta_s = \frac{\eta_{sca}}{\Delta m}, \quad \eta_t = \frac{\eta_{ten}}{\Delta m \tilde{r}_+^{s+2}}, \quad (9.6)$$

$$\mathcal{T} = \frac{\Delta t}{\Delta m + \Delta m_-} \tilde{r}^s, \quad (9.7)$$

$$P_{nv} = P_e + P_i + \frac{B^2}{8\pi} + \frac{1}{3} a_{SB} T_r^4 + \frac{2}{3} (\mathcal{E}_\alpha + \mathcal{E}_{p3} + \mathcal{E}_{p14}). \quad (9.8)$$

The boundary conditions are fulfilled as follows.

Left boundary, $j = 1$:

a) “center”, IFLBND=0:

$$A_1 = B_1 = 0; \quad (9.9)$$

at $j = 2$ in this case it is assumed that $A_- / \tilde{r}_- = 0$ and $(u_- + B_-) / \tilde{r}_- = 0$;

b) “closed cavity”, IFLBND=1:

$$\Delta m_- = 0, \quad \eta_{sca-} = \eta_{ten-} = 0, \quad (9.10)$$

$$P_{nv-} = P_{bl}(t + \frac{1}{2}\Delta t) + \frac{B_1^2}{8\pi} + \frac{1}{3} a_{SB} T_{r,1}^4 + \frac{2}{3} (\mathcal{E}_{\alpha,1} + \mathcal{E}_{p3,1} + \mathcal{E}_{p14,1});$$

here $B_1, T_{r,1}, \mathcal{E}_{\alpha,1}, \mathcal{E}_{p3,1}, \mathcal{E}_{p14,1}$ are the values of corresponding quantities in the first (from the left) mesh cell, i.e. at $j = 1$;

c) “open halfspace”, IFLBND=-1:

$$\Delta m_- = 0, \quad \eta_{sca-} = \eta_{ten-} = 0, \quad (9.11)$$

$$P_{nv-} = P_{bl}(t + \frac{1}{2}\Delta t) + \frac{B_{bl}^2(t + \frac{1}{2}\Delta t)}{8\pi} + \frac{1}{3} a_{SB} T_{rlex}^4(t + \frac{1}{2}\Delta t).$$

Right boundary, $j = N + 1$:

$$\Delta m = 0, \quad \eta_{sca} = \eta_{ten} = 0, \quad (9.12)$$

$$P_{nv} = P_{br}(t + \frac{1}{2}\Delta t) + \frac{B_{br}^2(t + \frac{1}{2}\Delta t)}{8\pi} + \frac{1}{3} a_{SB} T_{rex}^4(t + \frac{1}{2}\Delta t);$$

in particular, this implies $A_{N+1} = 0, \bar{u}_{N+1} = B_{N+1}$. Once the coefficients $A \equiv A_j, B \equiv B_j$ ($j = 1, \dots, N+1$) are calculated, the values of $\bar{u} \equiv \bar{u}_j$ are obtained through a recursive run in the opposite direction from Eq. (9.1).

In the process of solving for \bar{u} , the values of \dot{V} and of the viscous heating $\eta_{sca}(\dot{V})^2 + \eta_{ten}(\Sigma)^2$ are calculated as well; the latter is added to the ion heating Q_i , while the values of \dot{V} are memorized to be used when solving Eqs (8.3)–(8.7).

3) The new radii are found from

$$\bar{r} = \tilde{r} + \frac{1}{2} \bar{u} \Delta t, \quad (9.13)$$

while the new values of the specific volume \bar{V} are calculated from Eq. (8.28); the old values V are being kept until exiting UPSLOI.

If the ‘‘closed cavity’’ boundary condition is chosen initially, the central void cavity may close in the process of implosion, i.e. the inner (left) radius r_1 of the target — which initially must be positive — may reach the value $r_1 = 0$. We use the following criterion of void closure: the void cavity closes at a given time step if

$$\tilde{r}_1 = r_1 + \frac{1}{2} u_1 \Delta t \leq \frac{1}{2} r_1, \quad \text{or} \quad \bar{r}_1 = \tilde{r}_1 + \frac{1}{2} \bar{u}_1 \Delta t \leq 0.01 \tilde{r}_1. \quad (9.14)$$

Once this criterion is fulfilled, the value of IFLBND is changed from IFLBND=1 to IFLBND=0, the values of \bar{r}_1 and \bar{u}_1 are set equal to $\bar{r}_1 = \bar{u}_1 = 0$, and the amount of kinetic energy $\frac{1}{4} \Delta m_1 u_1^2$ is added to the ion component of the internal energy by assigning

$$Q_{i,1} = Q_{i,1} + \frac{1}{4} u_1^2 / \Delta t. \quad (9.15)$$

III. Block NEWREAL. In this block the linear equations (8.7) for the energy density $\bar{\mathcal{E}}_{(\alpha)}$ of fast fusion products are solved. Each of the three diffusion equations is solved independently from the other two according to the following scheme. First of all we note that the necessary boundary conditions (see section 4) will be fulfilled after we rewrite Eq. (8.7) as

$$\begin{aligned} & \bar{V} \bar{\mathcal{E}}_{(\alpha)} - V \mathcal{E}_{(\alpha)} + \frac{2}{3} \Delta t \dot{V} \mathcal{E}_{(\alpha)} + \Delta t \chi_{(\alpha)} \bar{\mathcal{E}}_{(\alpha)} = \\ & = \Delta t Q_{(\alpha)} + \frac{\Delta t}{\Delta m} \left\{ \begin{array}{ll} 0, & j = 1 \wedge \text{IFLBND} = 0, 1, \\ -\frac{2d_{(\alpha)}}{\bar{r}_+ - \bar{r}} \bar{\mathcal{E}}_{(\alpha)}, & j = 1 \wedge \text{IFLBND} = -1, \\ \bar{r}^s \frac{d_{(\alpha)-} + d_{(\alpha)}}{\bar{r}_+ - \bar{r}_-} (\bar{\mathcal{E}}_{(\alpha)-} - \bar{\mathcal{E}}_{(\alpha)}), & j > 1, \end{array} \right\} - \\ & - \frac{\Delta t}{\Delta m} \left\{ \begin{array}{ll} \bar{r}^s \frac{d_{(\alpha)} + d_{(\alpha)+}}{\bar{r}_{+2} - \bar{r}} (\bar{\mathcal{E}}_{(\alpha)} - \bar{\mathcal{E}}_{(\alpha)+}), & j < N, \\ \bar{r}^s \frac{2d_{(\alpha)}}{\bar{r}_+ - \bar{r}} \bar{\mathcal{E}}_{(\alpha)}, & j = N. \end{array} \right\} \end{aligned} \quad (9.16)$$

Once we introduce a representation

$$\bar{\mathcal{E}}_{(\alpha)} = A_{(\alpha)} \bar{\mathcal{E}}_{(\alpha)+} + B_{(\alpha)}, \quad (9.17)$$

we can calculate the coefficients $A_{(\alpha)}$ and $B_{(\alpha)}$ from the following recurrent formulae,

$$A_{(\alpha)} = \frac{F_{(\alpha)+}}{\Delta m \Omega_{(\alpha)}}, \quad (9.18)$$

$$B_{(\alpha)} = \frac{1}{\Omega_{(\alpha)}} \left[V \mathcal{E}_{(\alpha)} + \Delta t \left(Q_{(\alpha)} - \frac{2}{3} \mathcal{E}_{(\alpha)} \dot{V} \right) + \left\{ \begin{array}{ll} 0, & j = 1, \\ \frac{F_{(\alpha)} B_{(\alpha)-}}{\Delta m}, & j > 1, \end{array} \right\} \right], \quad (9.19)$$

$$\Omega_{(\alpha)} = \bar{V} + \Delta t \chi_{(\alpha)} + \left\{ \begin{array}{ll} 0, & j = 1 \wedge \text{IFLBND} = 0, 1, \\ \frac{\Delta t}{\Delta m} \frac{2d_{(\alpha)}}{\bar{r}_+ - \bar{r}}, & j = 1 \wedge \text{IFLBND} = -1, \\ \frac{F_{(\alpha)} (1 - A_{(\alpha)-})}{\Delta m}, & j > 1, \end{array} \right\} +$$

$$+ \left\{ \begin{array}{ll} \frac{F_{(\alpha)+}}{\Delta m}, & j < N, \\ \frac{\Delta t}{\Delta m} \bar{r}_+^s \frac{2d_{(\alpha)}}{\bar{r}_+ - \bar{r}}, & j = N, \end{array} \right\} \quad (9.20)$$

$$F_{(\alpha)} = \bar{r}^s \frac{\Delta t}{\bar{r}_+ - \bar{r}_-} (d_{(\alpha)-} + d_{(\alpha)}). \quad (9.21)$$

Once the values of $A_{(\alpha)}$ and $B_{(\alpha)}$ are calculated, one obtains $\bar{\mathcal{E}}_{(\alpha)}$ from Eq. (9.17). The boundary conditions are satisfied by setting either $\bar{\mathcal{E}}_{(\alpha),N+1} = 0$ or $F_{(\alpha),N+1} = 0$.

After the values of $\bar{\mathcal{E}}_{(\alpha)}$ have been found, the energy dissipation rates $\chi_{e(\alpha)}\bar{\mathcal{E}}_{(\alpha)}$ and $\chi_{i(\alpha)}\bar{\mathcal{E}}_{(\alpha)}$ are added to the electron and ion heating rates Q_e and Q_i , respectively.

IV. Block NEWHZ. In this block the diffusion equation (8.6) for the magnetic field \bar{B} is solved. To satisfy explicitly the boundary conditions, we rewrite it as

$$\begin{aligned} \bar{B}\bar{V} - BV = \frac{\Delta t}{\Delta m} & \left\{ \begin{array}{ll} 0, & j = 1 \wedge \text{IFLBND} = 0, 1, \\ \frac{c^2}{4\pi} \frac{2\eta_{\perp}}{\bar{r}_+ - \bar{r}} (\bar{B}_{bl} - \bar{B}), & j = 1 \wedge \text{IFLBND} = -1, \\ \frac{c^2}{4\pi} \bar{r}^s \frac{\eta_{\perp-} + \eta_{\perp}}{\bar{r}_+ - \bar{r}_-} (\bar{B}_- - \bar{B}), & j > 1, \end{array} \right\} - \\ & - \frac{\Delta t}{\Delta m} \left\{ \begin{array}{ll} \frac{c^2}{4\pi} \bar{r}_+^s \frac{\eta_{\perp} + \eta_{\perp+}}{\bar{r}_{+2} - \bar{r}} (\bar{B} - \bar{B}_+), & j < N, \\ \frac{c^2}{4\pi} \bar{r}_+^s \frac{2\eta_{\perp}}{\bar{r}_+ - \bar{r}} (\bar{B} - \bar{B}_{br}), & j = N, \end{array} \right\}. \end{aligned} \quad (9.22)$$

Once we introduce a representation

$$\bar{B} = \mathcal{A}\bar{B}_+ + \mathcal{B}, \quad (9.23)$$

we can calculate the coefficients \mathcal{A} and \mathcal{B} from the following recurrent formulae,

$$\mathcal{A} = \left\{ \begin{array}{ll} \frac{F_+}{\Delta m \Omega}, & j < N, \\ \frac{c^2}{4\pi} \frac{\Delta t}{\Delta m \Omega} \bar{r}_+^s \frac{2\eta_{\perp}}{\bar{r}_+ - \bar{r}}, & j = N, \end{array} \right\} \quad (9.24)$$

$$\mathcal{B} = \frac{1}{\Omega} \left[BV + \left\{ \begin{array}{ll} 0, & j = 1 \wedge \text{IFLBND} = 0, 1, \\ \frac{c^2}{4\pi} \frac{\Delta t}{\Delta m} \frac{2\eta_{\perp}}{\bar{r}_+ - \bar{r}} B_{bl}, & j = 1 \wedge \text{IFLBND} = -1, \\ \frac{F\mathcal{B}_-}{\Delta m}, & j > 1, \end{array} \right\} \right], \quad (9.25)$$

$$\begin{aligned} \Omega = \bar{V} + & \left\{ \begin{array}{ll} 0, & j = 1 \wedge \text{IFLBND} = 0, 1, \\ \frac{c^2}{4\pi} \frac{\Delta t}{\Delta m} \frac{2\eta_{\perp}}{\bar{r}_+ - \bar{r}}, & j = 1 \wedge \text{IFLBND} = -1, \\ \frac{F(1 - \mathcal{A}_-)}{\Delta m}, & j > 1, \end{array} \right\} + \\ & + \left\{ \begin{array}{ll} \frac{F_+}{\Delta m}, & j < N, \\ \frac{c^2}{4\pi} \frac{\Delta t}{\Delta m} \bar{r}_+^s \frac{2\eta_{\perp}}{\bar{r}_+ - \bar{r}}, & j = N, \end{array} \right\}, \end{aligned} \quad (9.26)$$

$$F = \frac{c^2}{4\pi} \bar{r}^s \frac{\Delta t}{\bar{r}_+ - \bar{r}_-} (\eta_{\perp-} + \eta_{\perp}). \quad (9.27)$$

Once the values of \mathcal{A} and \mathcal{B} are calculated, one obtains \bar{B} from the recurrent formula(9.23). The boundary condition at the right boundary is satisfied by setting $B_{N+1} = B_{br}$.

V. Block NEWTTT. In this block, three coupled systems of linear equations (8.3)–(8.5) for \bar{T}_e , \bar{T}_i , and \bar{T}_r are solved. First of all, to fulfill the boundary conditions for radiation diffusion, we rewrite Eq. (8.5) in the form

$$4 a_{SB} T_r^3 \bar{V} (\bar{T}_r - T_r) + a_{SB} T_r^4 \left(\bar{V} - V + \frac{1}{3} \dot{V} \Delta t \right) = \chi_{er} (\bar{T}_e - \bar{T}_r) \Delta t +$$

$$+ \left\{ \begin{array}{ll} 0, & j = 1 \wedge \text{IFLBNB} = 0, 1; \\ \frac{ca_{SB}}{4} \frac{\Delta t}{\Delta m} (T_{rlex}^4 - T_r^3 \bar{T}_r), & j = 1 \wedge \text{IFLBNB} = -1; \\ \bar{r}^s \frac{\Delta t}{\Delta m} \frac{2\hat{\kappa}_r^*}{(\bar{r}_+ - \bar{r}_-)} (\bar{T}_{r-} - \bar{T}_r), & j > 1, \end{array} \right\} -$$

$$- \left\{ \begin{array}{ll} \bar{r}_+^s \frac{\Delta t}{\Delta m} \frac{2\hat{\kappa}_{r+}^*}{(\bar{r}_{+2} - \bar{r})} (\bar{T}_r - \bar{T}_{r+}), & j < N, \\ \frac{ca_{SB}}{4} \bar{r}_+^s \frac{\Delta t}{\Delta m} (T_r^3 \bar{T}_r - T_{rex}^4), & j = N, \end{array} \right\}. \quad (9.28)$$

Then, we cast Eqs (8.3), (8.4), and (9.28) in the matrix form

$$\|G\| \cdot \|\bar{T}\| = \|F_+\| \cdot \|\bar{T}_+\| + \|Q\|, \quad (9.29)$$

where

$$\|\bar{T}\| = \begin{Bmatrix} \bar{T}_e \\ \bar{T}_r \\ \bar{T}_i \end{Bmatrix}, \quad \|G\| = \begin{Bmatrix} G_{11} & G_{12} & G_{13} \\ G_{21} & G_{22} & G_{23} \\ G_{31} & G_{32} & G_{33} \end{Bmatrix},$$

$$\|Q\| = \begin{Bmatrix} Q_1 \\ Q_2 \\ Q_3 \end{Bmatrix}, \quad \|F_+\| = \begin{Bmatrix} F_{e+} & 0 & 0 \\ 0 & F_{r+} & 0 \\ 0 & 0 & F_{i+} \end{Bmatrix}. \quad (9.30)$$

Solution to Eq. (9.29) is obtained by assuming a representation

$$\|\bar{T}\| = \|A\| \cdot \|\bar{T}_+\| + \|B\|, \quad (9.31)$$

and using the following recurrence relations

$$\|A\| = \|G\|^{-1} \cdot \|F_+\|, \quad \|B\| = \|G\|^{-1} \cdot \|Q\|, \quad (9.32)$$

to calculate the matrices $\|A\|$ and $\|B\|$. Here

$$G_{11} = \epsilon_e T + \chi_{er} \Delta t + \chi_{ei} \Delta t + F_e (1 - A_{11-}) + F_{e+}, \quad (9.33)$$

$$G_{12} = -\chi_{er} \Delta t - F_e A_{12-}, \quad (9.34)$$

$$G_{13} = -\chi_{ei} \Delta t - F_e A_{13-}, \quad (9.35)$$

$$G_{21} = -\chi_{er} \Delta t - \left\{ \begin{array}{ll} 0, & j = 1, \\ F_r A_{21-}, & j > 1, \end{array} \right\}, \quad (9.36)$$

$$G_{22} = 4a_{SB} T_r^3 \bar{V} + \chi_{er} \Delta t + \left\{ \begin{array}{ll} 0, & j = 1 \wedge \text{IFLBND} = 0, 1, \\ \frac{ca_{SB}}{4} \frac{\Delta t}{\Delta m} T_r^3, & j = 1 \wedge \text{IFLBND} = -1, \\ F_r (1 - A_{22-}), & j > 1, \end{array} \right\} + \left\{ \begin{array}{ll} F_{r+}, & j < N, \\ \frac{ca_{SB}}{4} \bar{r}_+^s \frac{\Delta t}{\Delta m} T_r^3, & j = N, \end{array} \right\}, \quad (9.37)$$

$$G_{23} = \left\{ \begin{array}{ll} 0, & j = 1, \\ -F_r A_{23-}, & j > 1, \end{array} \right\}, \quad (9.38)$$

$$G_{31} = -\chi_{ei} \Delta t - F_i A_{31-}, \quad (9.39)$$

$$G_{32} = -F_i A_{32-}, \quad (9.40)$$

$$G_{33} = \epsilon_{iT} + \chi_{ei} \Delta t + F_i (1 - A_{33-}) + F_{i+}, \quad (9.41)$$

$$Q_1 = \epsilon_{eT} T_e + Q_e \Delta t + F_e B_{1-}, \quad (9.42)$$

$$Q_2 = a_{SB} T_r^4 (3\bar{V} + V - \frac{1}{3} \dot{V} \Delta t) + \left\{ \begin{array}{ll} 0, & j = 1 \wedge \text{IFLBND} = 0, 1, \\ \frac{ca_{SB}}{4} \frac{\Delta t}{\Delta m} T_{rlex}^4, & j = 1 \wedge \text{IFLBND} = -1, \\ F_r B_{2-}, & j > 1, \end{array} \right\} + \left\{ \begin{array}{ll} 0, & j < N, \\ \frac{ca_{SB}}{4} \frac{\Delta t}{\Delta m} \bar{r}_+^s T_{rex}^4, & j = N, \end{array} \right\}, \quad (9.43)$$

$$Q_3 = \epsilon_{iT} T_i + Q_i \Delta t + F_i B_{3-}, \quad (9.44)$$

$$F_e = \bar{r}^s \frac{\Delta t}{\bar{r}_+ - \bar{r}_-} \frac{2\hat{k}_e^*}{\Delta m}, \quad F_r = \bar{r}^s \frac{\Delta t}{\bar{r}_+ - \bar{r}_-} \frac{2\hat{k}_r^*}{\Delta m}, \quad F_i = \bar{r}^s \frac{\Delta t}{\bar{r}_+ - \bar{r}_-} \frac{2\hat{k}_i^*}{\Delta m}. \quad (9.45)$$

In addition, we set

$$F_{e,1} = F_{i,1} = F_{e,N+1} = F_{i,N+1} = F_{r,N+1} = 0 \quad (9.46)$$

to satisfy the boundary conditions. Once the matrix arrays $\|A\|$ and $\|B\|$ are calculated (note that at each recursive step we have to invert matrix $\|G\|$), the arrays \bar{T}_e , \bar{T}_i , and \bar{T}_r are found in a reverse recursive run from Eq. (9.31).

10 EVALUATION OF THE TIME STEP

The numerical algorithm implemented in the DEIRA code does not allow to return to the “old” values of the principal variables (3.20) after the “new” ones have been obtained in the case when too large a time step Δt has been chosen. Hence, a special attention should be paid to the procedure of evaluation of the next value of Δt . This procedure is realized in the subroutine STEP. It incorporates the following upper bounds on the value of Δt .

- 1) For the explicit method (8.2) of solving the hydrodynamic equation of motion to be numerically stable,

the time step Δt should be restricted by the condition [24]

$$\Delta t \leq K_h \min \left\{ \frac{1}{2} \frac{r_{N+1} - r_N}{[(P_b - P_{e,N} - P_{i,N})V_N]^{1/2}}; \Delta t_C \right\}, \quad (10.1)$$

where

$$\Delta t_C = \min_j \left\{ \frac{r_+ - r}{u_s (1 + \mu_{1av,sc} + \mu_{1av,tn})}; \frac{1}{4} \frac{r_+ - r}{|u_+ - u| (\mu_{2av,sc} + \mu_{2av,tn})} \right\}, \quad (10.2)$$

u_s is the adiabatic sound velocity [see Eq. (5.10)], and $0 < K_h < 1$ is the safety coefficient. The second term on the r.h.s. of Eq. (10.2) is evaluated only during compression, when $u > u_+$.

2) Since energy equations (8.3), (8.4) contain “old” values of all the heating rates and heat capacities, an additional restriction on the value of Δt is needed to avoid large errors in simulating fast thermal flares. As such, we have adopted the condition

$$\Delta t \leq K_Q \frac{\epsilon_{min} + \epsilon_{eT} T_e + \epsilon_{iT} T_i}{|Q_{ecl} + Q_{en} + Q_{dr}| + |Q_{icl} + Q_{in}| + \chi_\alpha \mathcal{E}_\alpha + \chi_{p3} \mathcal{E}_{p3} + \chi_{p14} \mathcal{E}_{p14}}, \quad (10.3)$$

where ϵ_{min} is a constant setting the “energy sensitivity threshold”, K_Q is a safety coefficient whose typical values are $K_Q \simeq 0.1$ – 0.2 .

3) For fixed values of the heat capacities, diffusion and relaxation coefficients, the conditions of numerical stability of the diffusion and relaxation terms in Eqs (8.3)–(8.7) impose no restrictions on the value of Δt . On the other hand, within the framework of our numerical scheme, strongly non-linear heat and radiation waves with steep temperature gradients can propagate no faster than one mesh interval in one time step. Clearly, adequate simulation of such waves requires an additional restriction on possible values of Δt . We introduce the corresponding upper bound for Δt by simply correcting the previous value of the time step Δt_- :

$$\frac{\Delta t}{\Delta t_-} \leq \begin{cases} 1 + K_\Delta, & \delta < K_{VT}/(1 + K_\Delta), \\ 1, & K_{VT}/(1 + K_\Delta) < \delta < K_{VT}(1 + K_\Delta) \\ \frac{K_{VT}}{\delta}, & K_{VT}(1 + K_\Delta) < \delta. \end{cases} \quad (10.4)$$

Here $K_\Delta \simeq 0.1$ – 0.2 sets an upper limit for a possible increment of Δt in a single time step, K_{VT} is the upper limit for possible relative changes of V , T_e , T_i , and T_r in a single time step. The quantity δ is defined as

$$\delta = \max\{\delta_V; \delta_{T_e}; \delta_{T_i}; \delta_{T_r}\}, \quad (10.5)$$

$$\delta_V = \max_j \left\{ \max \left\{ \frac{\bar{V}}{V}; \frac{V}{\bar{V}} \right\} - 1 \right\}, \quad (10.6)$$

$$\delta_{T_e} = \max_j \left\{ \max \left\{ \frac{\max\{\bar{T}_e; T_{min}\} + T_{min}}{T_e + T_{min}}; \frac{T_e + T_{min}}{\max\{\bar{T}_e; T_{min}\} + T_{min}} \right\} - 1 \right\}. \quad (10.7)$$

Maximum relative changes of the ion, δ_{T_i} , and radiation, δ_{T_r} , temperatures are defined analogously to δ_{T_e} . Note that condition (10.4) allows the value of Δt to decrease arbitrarily sharply and to increase only gradually.

It should be mentioned here that in some cases, when temperature jumps are present in the initial conditions or some processes are “turned on” abruptly, the step correction procedure (10.4) cannot prevent from a few “bad” steps. Also, when certain transport coefficients are too strong functions of their arguments, this procedure may become weakly unstable. Otherwise, in most practical cases it proved to be quite adequate in keeping the discretization errors at a sufficiently low level.

11 BLOCK SCHEME OF THE DEIRA CODE

The principal block scheme of the DEIRA code is shown in Fig. 2. It displays the following sequence of calculations. After the main run parameters have been assigned, the subroutine `START` is invoked to construct the numerical mesh and to assign the initial values to all the principal variables. Then, between the starting (A) and the ending (B) points of the main loop, the principal variables are recalculated to a new time moment. First, `URSOS` calculates all the necessary thermodynamic functions. Next, the external energy input Q_{dr} is calculated in the subroutine `DRIVE`. After that, `KINBUR` calculates all the transport and relaxation coefficients, thermonuclear burn rates, and electron ($Q_{ecl} + Q_{en}$) and ion ($Q_{icl} + Q_{in}$) components of the local heating by the charged fusion products and by fast neutrons. Subroutine `STEP` evaluates the time step Δt to be made. In `EBALNC`, corresponding increments are added to various components of the liberated thermonuclear energy. And, finally, the “new” values of the principal dependent variables are calculated in the subroutine `UPSLOI`. After that, the control is returned back to point A and the whole cycle is repeated for a new time step. Note that the sequential order of the subroutine calls shown in Fig. 2 is essential and must not be changed.

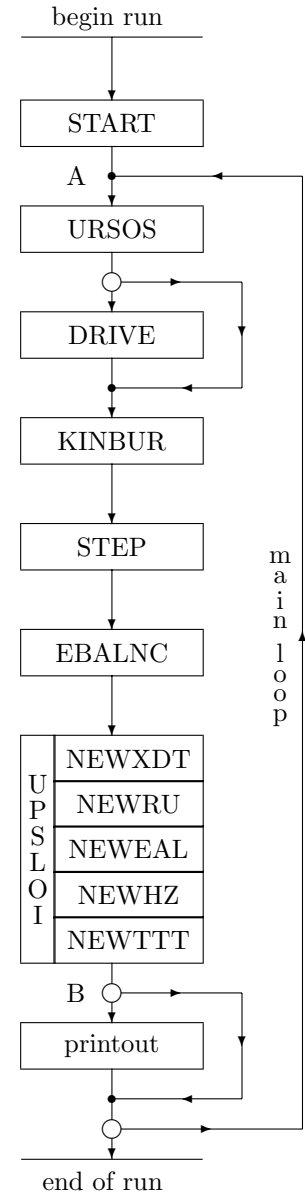


Figure 2.

12 TEST PROBLEMS

In test simulations, the numerical results from the DEIRA code have been compared with analytic and self-similar solutions for one or several equations from the full system (3.1)–(3.14). The test problems can be grouped according to the specific physical processes under trial.

12.1 Hydrodynamics

The basic set of test problems for hydrodynamics is described in Ref. [3]. Test runs have been performed for the Guderley solution (in cylindrical and spherical geometries), for a planar piston with reflection of the shock wave from the rigid wall, for the problem of homologous compression and expansion of a sphere. On the basis of these tests, the values of the six free parameters of the artificial viscosity have been chosen. In addition, a test run has been performed for the self-similar solution of a planar shock with heat conduction. The agreement with the exact solution was no worse than that observed earlier for the GITTAM code [25].

In all the above tests, an infinitely fast relaxation between the electron and ion temperatures has been

assumed. To test the process of temperature relaxation, the following version of the planar piston problem has been simulated. An ideal-gas equation of state of the form

$$P_e = \frac{1}{2} \rho T_e, \quad P_i = \frac{1}{2} \rho T_i, \quad \epsilon_e = \frac{T_e}{2(\gamma - 1)}, \quad \epsilon_i = \frac{T_i}{2(\gamma - 1)}, \quad (12.1)$$

is assumed; the electron-ion relaxation coefficient χ_{ei} is assumed to be constant, while the coefficients χ_{er} , κ_e , and κ_r are all set to zero. The initial state of the gas with $\gamma = 5/3$ in the region $0 \leq r \leq R_0 = 1$ is taken as

$$\rho(0, r) = \rho_0 = 1, \quad T_e(0, r) = T_i(0, r) = 0. \quad (12.2)$$

Starting from $t = 0$, a constant pressure P_1 is applied to the right boundary such that a strong shock propagates to the left with the speed $D = -1$. Gas parameters behind this shock are given by

$$\rho_1 = \frac{\gamma + 1}{\gamma - 1} \rho_0 = 4, \quad P_1 = \frac{2}{\gamma + 1} \rho_0 D^2 = \frac{3}{4}, \quad (12.3)$$

$$T_1 \equiv \frac{1}{2} (T_e + T_i)_1 = \frac{2(\gamma - 1)}{(\gamma + 1)^2} D^2 = \frac{3}{16}, \quad (12.4)$$

$$T_e = T_1 \left\{ 1 - \exp \left[-\frac{4(\gamma + 1)}{D} \chi_{ei} (r - r_0) \right] \right\}, \quad (12.5)$$

$$T_i = T_1 \left\{ 1 + \exp \left[-\frac{4(\gamma + 1)}{D} \chi_{ei} (r - r_0) \right] \right\}, \quad (12.6)$$

where $r_0 = R_0 - Dt$ is the shock front position at time t . Comparison of the exact solution (12.5), (12.6) for $\chi_{ei} = 1$ with the DEIRA simulation on 40 mesh intervals at $t = 0.75$ is shown in Fig. 3.

Figure 3: Electron-ion temperature relaxation behind the shock front.

12.2 Electron Heat Conduction and Diffusion of Radiation

Propagation of heat and radiation waves has been tested against motionless background by using the self-similar solution for a planar heat wave entering the half-space with a fixed temperature at the outer boundary and a power-law temperature dependence of the heat conduction coefficient. In such a case, the equation of heat conduction is

$$\rho c_V \frac{\partial T}{\partial t} = \frac{\partial}{\partial r} \left(\kappa_0 T^n \frac{\partial T}{\partial r} \right), \quad (12.7)$$

where c_V is the heat capacity per unit mass at constant volume. By introducing the self-similar variables

$$\xi = \left(\frac{n + 1}{2} \frac{\rho c_V}{\kappa_0 T_0^n} \right)^{1/2} \frac{r}{\sqrt{t}}, \quad \tau = \frac{T}{T_0}, \quad (12.8)$$

Eq. (12.7) can be reduced to

$$\frac{d^2 \tau^{n+1}}{d\xi^2} + \xi \frac{d\tau}{d\xi} = 0. \quad (12.9)$$

This equation should be solved with the boundary conditions

$$\tau(0) = 1, \quad \tau(\xi_0) = 0, \quad (12.10)$$

augmented by the condition for evaluating ξ_0 . The latter can be obtained by integrating Eq. (12.9) and noticing that the product $\tau^n (d\tau/d\xi)$ must vanish at $\xi = \xi_0$ because the heat flux, proportional to $\tau^n (d\tau/d\xi)$, must be a continuous function of r :

$$\alpha \equiv \int_0^{\xi_0} \tau d\xi = -(n + 1) \left. \frac{d\tau}{d\xi} \right|_{\xi=0}. \quad (12.11)$$

The constants ξ_0 and α define the penetration depth

$$r_f = \xi_0 \left[\frac{2\kappa_0 T_0^n}{(n+1)\rho c_V} t \right]^{1/2} \quad (12.12)$$

and the energy

$$E \equiv \rho c_V \int_0^{r_f} T dr = \alpha T_0 \left(\frac{2\kappa_0 T_0^n \rho c_V}{n+1} t \right)^{1/2} \quad (12.13)$$

of the heat wave in the half-space. The values of these constants calculated for certain n are given in Table 6. To the accuracy of $\simeq 0.6\%$ one can write

$$\alpha \approx \left(\frac{n+1}{n+\pi/2} \right)^{1/2}, \quad 0 < n < \infty; \quad \xi_0 \approx \left(1 + \frac{\pi}{2n} \right)^{1/2}, \quad 1 < n < \infty. \quad (12.14)$$

Table 6: Eigenvalues for a self-similar heat wave into a planar wall.

n	1	2	3	4	5	6	7
ξ_0	1.616121	1.335363	1.231172	1.176523	1.142817	1.119935	1.103380
α	0.887496	0.922297	0.940688	0.952049	0.959760	0.965336	0.969556

Three different types of heat waves have been tested corresponding to the following combinations of the transport coefficients:

1) electron conductivity wave with

$$\kappa_e = \kappa_{e0} T_e^3, \quad \kappa_r = \chi_{er} = 0; \quad (12.15)$$

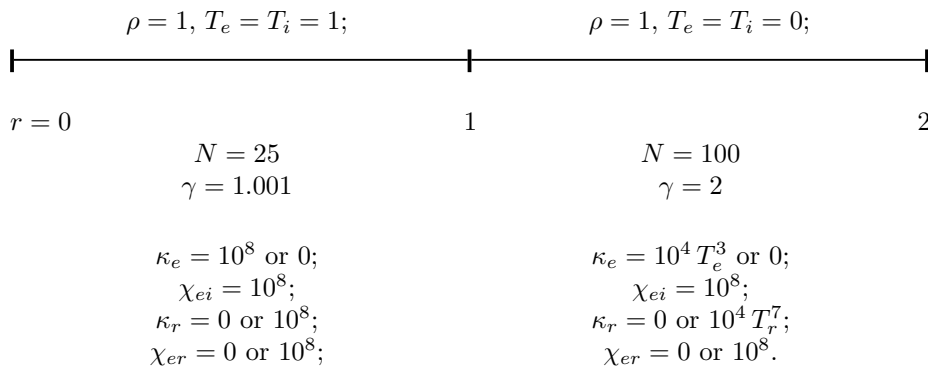
2) radiation heat wave with

$$\kappa_e = \chi_{er} = 0, \quad \kappa_r = \kappa_{r0} T_r^7; \quad (12.16)$$

3) electron-radiation heat wave with

$$\kappa_e = \kappa_{e0} T_e^3, \quad \kappa_r = 10^3 \kappa_{e0} T_r^3, \quad \chi_{er} = \infty. \quad (12.17)$$

In practice, these tests have been realized as different variants of the following planar target with the equation of state from Eq. (12.1) and $a_{SB} = 10^{-4}$:



In all cases, a good agreement between the DEIRA results and the analytic solutions have been observed, with the errors in the front propagation velocities not exceeding 1–2%.

12.3 Diffusion of the Energy of Fast Fusion Products

The diffusion equations for the energy density of three charged species of the fast fusion products have been tested against the following three problems.

1. Non-stationary diffusion. Consider a motionless gas slab in the region $0 < r < 1$ with constant values of ρ , χ_α , and d_α . In the absence of the source term ($Q_\alpha = 0$), the diffusion equation (3.9) takes the form

$$\frac{\partial \mathcal{E}_\alpha}{\partial t} + \rho \chi_\alpha \mathcal{E}_\alpha = d_\alpha \frac{\partial^2 \mathcal{E}_\alpha}{\partial r^2}. \quad (12.18)$$

This equation has a partial solution

$$\mathcal{E}_\alpha = C_\alpha \exp \left[- \left(\rho \chi_\alpha + \frac{\pi^2 v_{0\alpha}^2}{32 \rho \chi_\alpha} \right) t \right] \cos \left(\frac{\pi}{2} r \right), \quad (12.19)$$

which satisfies the boundary conditions (4.3), (4.15). In Eq. (12.19), the relationship (7.97) between χ_α and d_α has been taken into account. Numerical simulations have been performed on a grid of 40 mesh zones for the ideal-gas equation of state (12.1) and the following initial state:

$$\rho(0, r) = 1, \quad T_e(0, r) = T_i(0, r) = 3 \times 10^{-7}, \quad \chi_\alpha = 1, \quad C_\alpha = 10^{-6}. \quad (12.20)$$

Under such conditions, the hydrodynamic motion can be neglected for times $t \leq 1$. At $t = 1$, the values of $\mathcal{E}_\alpha(t, r)$ calculated with the DEIRA code for $v_{0\alpha} = 4\sqrt{2}/\pi$ deviate from the exact solution (12.19) by no more than 0.4%

2. Stationary diffusion. Consider a stationary gaseous sphere of radius R with constant values of ρ , $\chi_{(\alpha)}$, and $d_{(\alpha)}$, inside which the source $Q_{(\alpha)}$ has a constant intensity. Beyond this sphere, the gas is assumed to be in the same state, but the source term vanishes, i.e. $Q_{(\alpha)} = 0$. Then, the equation of stationary diffusion

$$\frac{1}{r^2} \frac{\partial}{\partial r} \left(r^2 d_{(\alpha)} \frac{\partial \mathcal{E}_{(\alpha)}}{\partial r} \right) - \rho \chi_{(\alpha)} \mathcal{E}_{(\alpha)} + \rho Q_{(\alpha)} = 0 \quad (12.21)$$

has a solution

$$\mathcal{E}_{(\alpha)}(r) = \frac{Q_{(\alpha)}}{\chi_{(\alpha)}} \begin{cases} (1 - C \sinh \xi / \xi), & \xi < \xi_0, \\ D \exp(-\xi) / \xi, & \xi > \xi_0, \end{cases} \quad (12.22)$$

where

$$\begin{aligned} \xi &= \frac{\sqrt{8}}{v_{0(\alpha)}} \rho \chi_{(\alpha)} r, & \xi_0 &= \frac{\sqrt{8}}{v_{0(\alpha)}} \rho \chi_{(\alpha)} R, \\ C &= (1 + \xi_0) \exp(-\xi_0), & D &= \xi_0 \cosh \xi_0 - \sinh \xi_0. \end{aligned} \quad (12.23)$$

Simulations have been performed in the region $0 \leq r \leq 3$ with $R = 1$ (40 mesh zones at $r \leq 1$, and 60 between $1 < r \leq 3$). The initial data and the values of constants have been set as follows:

$$\begin{aligned} \chi_\alpha &= \frac{v_{0\alpha}}{\sqrt{8}}, \quad \chi_{p3} = \frac{v_{0p3}}{\sqrt{8}}, \quad \chi_{p14} = \frac{v_{0p14}}{\sqrt{8}}, \quad \rho(0, r) = 1, \\ T_e(0, r) &= T_i(0, r) = 10 \text{ keV}, \quad X_D = X_T = X_{He} = \begin{cases} 1, & 0 \leq r < 1, \\ 0, & 1 \leq r \leq 3. \end{cases} \end{aligned} \quad (12.24)$$

The hydrodynamics and the heating and cooling of plasma have been ‘‘turned off’’ artificially. The source terms Q_α , Q_{p3} , and Q_{p14} were calculated according to the formulae from section 6.2 (depletion of fuel has been turned off as well); for $v_{0\alpha}$, v_{0p3} , and v_{0p14} , the values from Table 3 have been used. Under such conditions, a steady state is reached within $\Delta t \lesssim 0.01$. Table 7 compares the values of \mathcal{E}_α , \mathcal{E}_{p3} , and \mathcal{E}_{p14} from the DEIRA simulation with those from the analytic solution (12.22) for $t = 0.485$ at three characteristic radii.

3. Adiabatic compression. In the limit of $\chi_\alpha = d_\alpha = 0$ and in the absence of sources ($Q_\alpha = 0$), Eq. (3.9) describes adiabatic compression of fast fusion products with the adiabatic index $\gamma_\alpha = 5/3$. In particular,

Table 7: Stationary-diffusion test for the energy densities of fast fusion products.

j	DEIRA simulation			analytic		
	\mathcal{E}_α	\mathcal{E}_{p3}	\mathcal{E}_{p14}	\mathcal{E}_α	\mathcal{E}_{p3}	\mathcal{E}_{p14}
1	2.2154	2.185×10^{-3}	3.221×10^{-3}	2.2102	2.180×10^{-3}	3.213×10^{-3}
40 ($r = 1$)	1.1348	1.119×10^{-3}	1.650×10^{-3}	1.1529	1.137×10^{-3}	1.676×10^{-3}
83 ($r = 2$)	0.1819	1.793×10^{-4}	2.644×10^{-4}	0.20995	2.070×10^{-4}	3.052×10^{-4}

when a strong shock passes through a gas with the equation of state (12.1), the energy density of fast products should jump by a factor

$$\left(\frac{\gamma+1}{\gamma-1}\right)^{\gamma_\alpha} = 10.08 \quad \text{for } \gamma = \frac{5}{3}$$

across the shock front. A corresponding test run has been done for a planar piston problem with $\chi_\alpha = v_{0\alpha} = 10^{-7}$; the results are shown in Fig. 4.

Figure 4: Adiabatic compression of \mathcal{E}_α across the shock front.

A Single-fluid dissipative MHD equations derived from the two-fluid Braginskii equations

I will write this chapter when I have time.

B Opacity model: version DEIRA-3

B.1 General formulae

In the approximation that radiation field has a locally Planckian spectrum with temperature T_r in the comoving reference frame, the transfer of radiation can be described by the diffusion equation

$$\begin{aligned} \frac{\partial \mathcal{E}_r}{\partial t} + \mathbf{u} \cdot \nabla \mathcal{E}_r + \frac{4}{3} \mathcal{E}_r \operatorname{div}(\mathbf{u}) &= \operatorname{div} \left(\frac{c l_R}{3} \nabla \mathcal{E}_r \right) + \\ &+ \int_0^\infty \tilde{k}_a(h\nu) [\mathcal{B}(\nu, T_e) - \mathcal{B}(\nu, T_r)] d\nu + \frac{4\sigma_T}{m_e c} n_e \mathcal{E}_r \cdot (T_e - T_r). \end{aligned} \quad (\text{B.1})$$

Here

$$\mathcal{E}_r \equiv \frac{1}{c} \int_0^\infty \mathcal{B}(\nu, T_r) d\nu = a_{SB} T_r^4 \quad (\text{B.2})$$

is the energy density of radiation in the comoving frame,

$$a_{SB} = \frac{4\sigma_{SB}}{c} = \frac{\pi^2}{15\hbar^3 c^3} = 1.372 \times 10^{14} \text{ ergs cm}^{-3} \text{ keV}^{-4}, \quad (\text{B.3})$$

with the σ_{SB} being the Stefan-Boltzmann constant, $\tilde{k}_a(h\nu)$ [cm^{-1}] is the absorption coefficient corrected for stimulated emission,

$$\mathcal{B}(\nu, T_r) = \frac{8\pi h\nu^3}{c^2} \frac{1}{\exp(h\nu/T_r) - 1} \quad (\text{B.4})$$

is 4π times the Planckian intensity. The last term on the right-hand side of Eq. (B.1) represents the Compton energy exchange between electrons and radiation; $\sigma_T = 6.652 \times 10^{-25} \text{ cm}^2$ is the Thomson scattering cross-section.

The Rosseland mean free path l_R is defined as

$$l_R = l_R(\rho, T_e, T_r) = \frac{\int_0^\infty \frac{1}{\sigma_T n_e + \tilde{k}_a(h\nu)} \frac{\partial \mathcal{B}(\nu, T_r)}{\partial T_r} d\nu}{\int_0^\infty \frac{\partial \mathcal{B}(\nu, T_r)}{\partial T_r} d\nu}. \quad (\text{B.5})$$

It can be written as

$$l_R = \int_0^\infty \frac{R(x) dx}{\sigma_T n_e + \tilde{k}_a(xT_r)}, \quad (\text{B.6})$$

where

$$x = \frac{h\nu}{T_r}, \quad R(x) = \frac{15}{4\pi^4} \frac{x^4 e^{-x}}{(1 - e^{-x})^2}. \quad (\text{B.7})$$

When calculating l_R , it is physically reasonable to include Compton scattering as an additive term in the opacity. In our case, l_R is assumed to be a function of two temperatures, T_e and T_r , while normally it is evaluated as a function of one temperature $T_e = T_r$ only. When just the values of $l_R(\rho, T_e)$ are available, one can take, as a first approximation, $l_R(\rho, T_e, T_r) = l_R(\rho, T_e)$ for all $T_r \neq T_e$. In the system of basic DEIRA equations, the radiative heat flux is written in the form

$$\frac{1}{3} c l_R \nabla \mathcal{E}_r = \frac{4}{3} c a_{SB} l_R T_r^3 \nabla T_r; \quad (\text{B.8})$$

accordingly, we define the coefficient of radiative heat conduction as

$$\kappa_r = \frac{4}{3} c a_{SB} l_R T_r^3. \quad (\text{B.9})$$

Next, define the radiation-matter temperature relaxation coefficient χ_{er} by writing

$$(T_e - T_r) \rho \chi_{er} = \int_0^\infty \tilde{k}_a(h\nu) [\mathcal{B}(\nu, T_e) - \mathcal{B}(\nu, T_r)] d\nu + \frac{4\sigma_T}{m_e c} n_e \mathcal{E}_r \cdot (T_e - T_r). \quad (\text{B.10})$$

From this we obtain

$$\begin{aligned} \chi_{er} &= \chi_{er}(\rho, T_e, T_r) = \frac{4\sigma_T}{m_e c} \frac{n_e}{\rho} a_{SB} T_r^4 + \frac{\int_0^\infty \tilde{k}_a(h\nu) \mathcal{B}(\nu, T_e) d\nu - \int_0^\infty \tilde{k}_a(h\nu) \mathcal{B}(\nu, T_r) d\nu}{\rho(T_e - T_r)} = \\ &= \frac{4\sigma_T}{m_e c} \frac{n_e}{\rho} a_{SB} T_r^4 + \frac{c a_{SB}}{\rho} \frac{T_e^4 \int_0^\infty \tilde{k}_a(xT_e) P(x) dx - T_r^4 \int_0^\infty \tilde{k}_a(xT_r) P(x) dx}{T_e - T_r}, \end{aligned} \quad (\text{B.11})$$

where

$$P(x) = \frac{15}{\pi^4} \frac{x^3 e^{-x}}{1 - e^{-x}}. \quad (\text{B.12})$$

The Planckian mean free path l_P is defined as

$$l_P = l_P(\rho, T_e) = \frac{\int_0^\infty \mathcal{B}(\nu, T_e) d\nu}{\int_0^\infty \tilde{k}_a(h\nu) \mathcal{B}(\nu, T_e) d\nu} = \left[\int_0^\infty \tilde{k}_a(xT_e) P(x) dx \right]^{-1}. \quad (\text{B.13})$$

When we want to evaluate $\chi_{er}(\rho, T_e, T_r)$ by simply using known values of $l_P(\rho, T_e)$, we can take as a first approximation

$$\chi_{er} = \frac{4\sigma_T}{m_e c} \frac{n_e}{\rho} a_{SB} T_r^4 + \frac{c a_{SB}}{\rho} \frac{T_e^3}{l_P}. \quad (\text{B.14})$$

When evaluating the absorption coefficient $\tilde{k}_a(h\nu)$, we take into account free-free, free-bound, and bound-bound transitions:

$$\tilde{k}_a(h\nu) = \tilde{\sigma}_a(h\nu) \frac{\rho}{A m_A} = \left[\tilde{\sigma}_{ph}(h\nu) + \frac{\overline{Z^2}_{mol}}{Z^2 X_{mol}} \tilde{\sigma}_{ff}(h\nu) \right] \frac{\rho}{A m_A}. \quad (\text{B.15})$$

Here $\tilde{\sigma}_{ph}(h\nu)$ is the sum of the free-bound and bound-bound absorption cross-sections, $\tilde{\sigma}_{ff}(h\nu)$ is the cross-section of free-free absorption by one average atom (ion) — both corrected for stimulated emission. When calculating $\tilde{\sigma}_{ff}(h\nu)$, we take into account the Fermi degeneracy of the ideal electron gas.

B.2 Basic formulae in the DEIRA units

In the DEIRA units ($[t] = 10^{-8}$ s, $[l] = 0.1$ cm, $[m] = 10^{-3}$ g, $[T] = 1$ keV) the basic formulae become

$$\kappa_r = 5484 l_R T_r^3, \quad (\text{B.16})$$

$$l_R = 16.6 \frac{\bar{A}}{\rho} \int_0^\infty \frac{R(x) dx}{\tilde{\sigma}_a(xT_r) + 0.6652 y Z_{mol}/(Z X_{mol})}, \quad (\text{B.17})$$

$$l_P = 16.6 \frac{\bar{A}}{\rho} \left[\int_0^\infty \tilde{\sigma}_a(xT_e) P(x) dx \right]^{-1}, \quad (\text{B.18})$$

$$\chi_{er} = 1.290 T_r^4 \frac{y Z_{mol}}{Z A_{mol}} + \frac{4113}{16.6 \bar{A}} \frac{T_e^4 \int_0^\infty \tilde{\sigma}_a(xT_e) P(x) dx - T_r^4 \int_0^\infty \tilde{\sigma}_a(xT_r) P(x) dx}{T_e - T_r}. \quad (\text{B.19})$$

Here the total absorption cross-section $\tilde{\sigma}_a(h\nu)$ is in barns (10^{-24} cm²); y is the degree of ionization in the average ion model.

B.3 General formulae for the absorption cross-section

We evaluate the absorption cross-section as

$$\tilde{\sigma}_a(h\nu) = \tilde{\sigma}_{ph}(h\nu) + \frac{\overline{Z^2}_{mol}}{Z^2 X_{mol}} \tilde{\sigma}_{ff}(h\nu), \quad (\text{B.20})$$

where $\tilde{\sigma}_{ff}(h\nu)$ is the free-free absorption cross-section by an average ion with atomic number Z , atomic mass \bar{A} , and ionization degree y (positive charge $+ye$).

B.3.1 Bound-bound and bound-free transitions

First of all we notice that in the average ion approximation the ionization degree $0 < y < Z$ is not an integer. We define an integer i such that

$$i - 1 \leq y < i; \quad i = 1, 2, \dots, Z. \quad (\text{B.21})$$

We assume further that only two ion species, i and $i + 1$, are present in plasma with fractional abundances $(i - y)$ and $[1 - (i - y)]$, respectively; $i = 1$ corresponds to a neutral atom, $i = Z$ — to a hydrogen-like ion. Then

$$\tilde{\sigma}_{ph}(h\nu) = (i - y) \tilde{\sigma}_{ph,i}(h\nu) + [1 - (i - y)] \tilde{\sigma}_{ph,i+1}(h\nu). \quad (\text{B.22})$$

For the photoabsorption cross-section by ion i we adopt a simple approximation

$$\tilde{\sigma}_{ph,i}(h\nu) = a_i \alpha a_0^2 \left(\frac{e^2/a_0}{I_i} \right)^3 \times \begin{cases} \frac{1}{b_i} \left(\frac{h\nu}{I_i} \right)^2, & h\nu \leq I_i, \\ \left[\left(\frac{h\nu}{I_i} \right)^3 + (b_i - 1) \left(\frac{h\nu}{I_i} \right) \right]^{-1}, & h\nu \geq I_i. \end{cases} \quad (\text{B.23})$$

Here $\alpha = e^2/\hbar c$ is the fine-structure constant, $a_0 = \hbar^2/m_e e^2$ is the Bohr radius, I_i is the ionization potential of ion i , and a_i and b_i are dimensionless fitting constants. Note that the dependence $\tilde{\sigma}_{ph,i} \propto \nu^2$ at $h\nu < I_i$ is close to the Thomas-Fermi asymptotical behavior $\sigma_{ph} \propto \nu^{7/3}$ in the limit of small frequencies [26]. We set the value of a_i equal to

$$a_i = \begin{cases} \frac{8\pi Z^4}{3\sqrt{3}}, & i = Z, \quad \text{H-like ion,} \\ \frac{16\pi Z^4}{3\sqrt{3}}, & i \leq Z - 1, \quad \text{He-like and higher ions,} \end{cases} \quad (\text{B.24})$$

to satisfy the Kramers asymptotical behavior for the photoabsorption by K-electrons in the limit $h\nu \gg e^2 Z^2/a_0$. To determine the value of b_i , we invoke the Thomas-Reiche-Kuhn sum rule

$$\int_0^\infty \tilde{\sigma}_{ph,i}(h\nu) d\nu = \frac{\pi e^2}{m_e c} (Z + 1 - i). \quad (\text{B.25})$$

This condition leads to the following equation for b_i

$$F(b_i) = \Lambda_i, \quad (\text{B.26})$$

where

$$\Lambda_i = \frac{a_i}{6\pi^2(Z + 1 - i)} \left(\frac{e^2/a_0}{I_i} \right)^2, \quad (\text{B.27})$$

and the function $F(x)$ is given by

$$F(x) = \left(\frac{1}{x} + \frac{3}{2} \frac{\ln x}{x - 1} \right)^{-1}. \quad (\text{B.28})$$

This function is monotonously increasing from $F(0) = 0$ to $F(\infty) = \infty$. For H-like ions, which have $I_Z = \frac{1}{2}e^2 Z^2/a_0$, we obtain

$$\Lambda_Z = \frac{16}{9\pi\sqrt{3}} = 0.32671, \quad b_Z = 0.7495. \quad (\text{B.29})$$

B.3.2 Free-free transitions

The cross-section of free-free absorption in a partially degenerate plasma, as derived in Ref. [5], is given by

$$\tilde{\sigma}_{ff}(h\nu) = \frac{16\pi}{3\sqrt{3}} \alpha a_0^2 \frac{(e^2/a_0)^2 T_e}{(h\nu)^3} \ln \left[\frac{1 + \exp(\mu_e/T_e)}{1 + \exp(\mu_e/T_e - h\nu/T_e)} \right] \langle y^2 \rangle g_{ff}, \quad (\text{B.30})$$

where μ_e is the chemical potential of free electrons, g_{ff} is the Gaunt factor, and

$$\langle y^2 \rangle = (i - y)(i - 1)^2 + [1 - (i - y)] i^2. \quad (\text{B.31})$$

The chemical potential μ_e can be evaluated from the approximate formula

$$\exp\left(\frac{\mu_e}{T_e}\right) \approx \frac{1 + \exp(E_F/T_e)}{1 + \frac{3}{2}\sqrt{\pi} (T_e/E_F)^{3/2}}, \quad (\text{B.32})$$

where

$$E_F = \frac{\hbar^2}{2m_e} (3\pi^2 n_e)^{2/3} \quad (\text{B.33})$$

is the Fermi energy of free electrons. Formula (B.32) has the correct asymptotical behavior in both the Fermi and Boltzmann limits; in the intermediate region its error does not exceed 6%. Even in the Born approximation, the Gaunt factor g_{ff} cannot be reduced to elementary functions; here we use an approximate expression from Ref. [5]

$$g_{ff} \approx \frac{\sqrt{3}}{\pi} \times \begin{cases} \ln \left[\frac{2\mu_e}{h\nu} \left(1 + \sqrt{1 - (h\nu/2\mu_e)^2} \right) \right], & h\nu < 2(\mu_e - 0.71T_e), \\ \ln \left[1 + 2\frac{0.71T_e}{h\nu} \left(1 + \sqrt{1 + h\nu/0.71T_e} \right) \right], & h\nu \geq 2(\mu_e - 0.71T_e). \end{cases} \quad (\text{B.34})$$

For $\mu_e \simeq T_e \simeq h\nu$, the error of Eq. (B.34) may be as high as 20%, but in the Boltzmann limit $\exp(\mu_e/T_e) \ll 1$ this error is below 5% over the entire frequency range.

B.4 Absorption cross-section in the DEIRA units

Having adopted the units $[\sigma] = 10^{-24} \text{ cm}^2$ for the cross-sections, and $[\varepsilon] \equiv [h\nu] = [I_i] = 1 \text{ keV}$ for the photon energies and ionization potentials, we obtain

$$\tilde{\sigma}_a(\varepsilon) = \tilde{\sigma}_{ph}(\varepsilon) + \frac{\overline{Z^2}_{mol}}{Z^2 X_{mol}} \tilde{\sigma}_{ff}(\varepsilon), \quad (\text{B.35})$$

$$\tilde{\sigma}_{ph}(\varepsilon) = (i - y)\tilde{\sigma}_{ph,i}(\varepsilon) + [1 - (i - y)]\tilde{\sigma}_{ph,i+1}(\varepsilon), \quad (\text{B.36})$$

$$\tilde{\sigma}_{ph,i}(\varepsilon) = 4.1174 \frac{a_i}{I_i^3} \times \begin{cases} \frac{1}{b_i} \left(\frac{\varepsilon}{I_i} \right)^2, & \varepsilon \leq I_i, \\ \left[\left(\frac{\varepsilon}{I_i} \right)^3 + (b_i - 1) \frac{\varepsilon}{I_i} \right]^{-1}, & \varepsilon \geq I_i, \end{cases} \quad (\text{B.37})$$

$$a_i = 4.8368 (2 - \delta_{iZ}) Z^4, \quad (\text{B.38})$$

$$F(b_i) = \Lambda_i = 1.2504 \times 10^{-5} \frac{a_i}{I_i^2 (Z + 1 - i)}, \quad (\text{B.39})$$

$$F(x) = \frac{x}{1 + \frac{3}{2} \frac{x \ln x}{x - 1}}; \quad (\text{B.40})$$

$$\tilde{\sigma}_{ff}(\varepsilon) = 1463.7 \frac{T_e}{\varepsilon^3} \ln \left[\frac{1 + \exp(\mu_e/T_e)}{1 + \exp(\mu_e/T_e) \exp(-\varepsilon/T_e)} \right] \langle y^2 \rangle g_{ff}, \quad (\text{B.41})$$

$$\langle y^2 \rangle = (i - y)(i - 1)^2 + [1 - (i - y)]i^2, \quad (\text{B.42})$$

$$g_{ff} = 0.55133 \times \begin{cases} \ln \left[\frac{2\mu_e}{\varepsilon} \left(1 + \sqrt{1 - (\varepsilon/2\mu_e)^2} \right) \right], & \varepsilon < 2(\mu_e - 0.71T_e), \\ \ln \left[1 + 2 \frac{0.71T_e}{\varepsilon} \left(1 + \sqrt{1 + \varepsilon/0.71T_e} \right) \right], & \varepsilon \geq 2(\mu_e - 0.71T_e), \end{cases} \quad (\text{B.43})$$

$$\exp\left(\frac{\mu_e}{T_e}\right) = \frac{1 + \exp(E_F/T_e)}{1 + 634.03 \frac{T_e^{3/2} Z A_{mol}}{\rho y Z_{mol}}}, \quad E_F = 0.0260 \left(\frac{\rho y Z_{mol}}{Z A_{mol}} \right)^{2/3}. \quad (\text{B.44})$$

References

- [1] BASKO, M.M., Teplofiz. Vys. Temper. **23** (1985) 483 (English translation: Sov. High Temper. **23** (1985) 388).
- [2] S. I. Braginskii, in *Reviews of Plasma Physics*, ed. M. A. Leontovich (Consultants Bureau, New York, 1965), Vol. 1, p. 205.
- [3] BASKO, M.M., Zh. Vychisl. Matem. i Matem. Fiz. **30** (1990) 176 (in Russian).
- [4] BASKO, M.M., Fiz. Plazmy **10** (1984) 1195 (English translation: Sov. J. Plasma Phys. **10** (1984) 689).
- [5] BASKO, M.M., Equations of One-Dimensional Radiative Hydrodynamics with Heat Conduction and Kinetics of Thermonuclear Burn, Preprint ITEP-145, Inst. of Theor. Exp. Physics, Moscow (1985) (in Russian).
- [6] FOWLER, W.A., CAUGHLAM, G.R., ZIMMERMAN, B.A., Ann. Rev. Astron. Ap. **13** (1975) 69.
- [7] LIBERMAN, M.A., VELIKOVICH, A.L., J. Plasma Physics **31** (1984) 369.
- [8] BASKO, M.M., Fiz. Plazmy **13** (1987) 967 (in Russian); Sov. J. Plasma Phys. **13** (1987) 558 (English translation).
- [9] IMSHENNIK, V.S., MIKHAILOV, I.N., BASKO, M.M., MOLODTSOV, S.V., Zh. Eksp. Teor. Fiz. **90** (1986) 1669 (in Russian); Sov. Phys. — JETP **63** (1986) 980 (English translation).
- [10] BOBROVA, N.A., SASOROV, P.V., Fiz. Plazmy **19** (1993) 789-795 (in Russian); Plasma Phys. Rep. **19**(6) (1993) 409-412 (English translation).
- [11] MAX, C.E., MCKEE, C.F., MEAD, W.C., Phys. Fluids **23** (8) (1980) 1620.
- [12] LEE, ...
- [13] LAMPE, M., Phys. Rev. **174** ...
- [14] LAMPE, M., Phys. Rev. **170** (1968) 306.
- [15] FERMI, E., TELLER, E., Phys. Rev. **72** (1947) 399.
- [16] BRYSK, H., Plasma Physics **16** (10) (1974) 927.
- [17] YAKOVLEV, D.G., URPIN, V.A., Astron. Zh. (Sov. Astronomy) **57** (3) (1980) 526 (in Russian).
- [18] BRYSK, H., CAMPBELL, P.M., HAMMERLING, P., Plasma Physics **17** (6) (1975) 473.
- [19] HUBBARD, W.B., LAMPE, M., Astrophys. J. Suppl. **18** No. 163 (1969) 297.
- [20] Seagrave J.D., Phys. Rev. **97** (1955) 757.
- [21] Kikuchi S., Sanada J., Suwa Sh., Hayashi I., Nisimura K., and Fukunaga K., , J. Phys. Soc. Jpn **15** (1960) 9.
- [22] Kootsey J.M., Nucl. Phys. A **113** (1968) 65.

- [23] Glöckle W., Witala H., Hüber D., Kamafda H., and Golak J., Phys. Rep. **274** (1996) 107.
- [24] RICHTMYER, R.D., MORTON, K.W., Difference Methods for Initial-Value Problems, Interscience Publ., New York (1967).
- [25] BASKO, M.M., SOKOLOVSKII, M.V., Preprint ITEP 89–89, Moscow (1989).
- [26] VINOGRADOV, A.V., TOLSTIKHIN, O.I., Preprint FIAN No. 139 (1989) (in Russian).
- [27] NEVINS, W.M., and SWAIN, R., Nucl. Fusion **40** (2000) 865.